The University of Manitoba

EFFECT OF SADDLE-POINT ANISOTROPY ON POINT-DEFECT DRIFT-DIFFUSION INTO STRAIGHT DISLOCATIONS

by

B.C. Skinner

A Thesis submitted to the Faculty of Graduate Studies in partial fulfillment of the requirements for the Degree of Master of Science through the Department of Physics.

The research work was conducted at the Materials Science Branch, Whiteshell Nuclear Research Establishment, Pinawa Manitoba ROE 1LO.

Winnipeg, Manitoba, 1983

EFFECT OF SADDLE-POINT ANISOTROPY ON POINT-DEFECT DRIFT-DIFFUSION INTO STRAIGHT DISLOCATIONS

by

Blair C. Skinner

A thesis submitted to the Faculty of Graduate Studies of the University of Manitoba in partial fulfillment of the requirements of the degree of

MASTER OF SCIENCE

CONTENTS

ABSTRACT

Effects on point-defect drift-diffusion in the strain fields of straight edge or screw dislocations, due to the anisotropy of the point defect in its saddle-point configuration, are investigated. Expressions for sink strength and bias that include the saddle-point shape effect are derived, both in the absence and presence of an externally applied stress. These are found to depend on intrinsic parameters such as the relaxation volume and the saddle-point shape of the point defects, and extrinsic parameters such as temperature and the magnitude and direction of the externally applied stress with respect to the line direction and Burgers vector direction of the dislocation.

The theory is applied to fcc copper and bcc iron. It is found that screw dislocations are biased sinks and that the stress-induced bias differential for the edge dislocations depends much more on the line direction than the Burgers vector direction. Comparison with the stress-induced bias differential due to the usual Stress Induced Preferred Absorption (SIPA) effect is made. It is found that the present effect causes a bias differential that is more than an order of magnitude larger.

ACKNOWLEDGEMENTS

This research has been supported by a Natural Sciences and Engineering Research Council Scholarship for which I am grateful.

Thanks to my wife, Janet and my son, Brett who were a source of strength and inspiration during the period of my studies.

I would like to thank Dr. R. Dutton for a critical reading of the manuscript and for his many useful suggestions.

Thanks to Lori Graham and Marg McDowall for their excellent contribution in the presentation of this thesis.

Special thanks to my supervisor, Dr. C.H. Woo who gave his time and energy to teach me basic materials science and the concepts used in irradiation damage studies.

Chapter 1

INTRODUCTION

When a sufficiently energetic particle collides with an atom of a crystalline material, the primary collision and subsequent cascade of collisions result in one or more atoms being displaced from their lattice sites. Equal numbers of vacancies and interstitials are created. As a result, the material contains concentrations of these point defects in excess of their respective thermal equilibrium concentrations. This provides a driving force for the point defects to come out of solution. At elevated temperatures the point defects are mobile and can combine with impurity atoms or point defects of the same type to nucleate point-defect clusters, or recombine with point defects of the opposite type, or annihilate at extended crystal defects such as voids, dislocation loops, network dislocations or grain boundaries. An extended crystal defect (or sink) will evolve if an excess of one type of point defect is absorbed by it. The evolution of the various sinks is believed to be the cause of the macroscopic deformation of a crystalline material subjected to irradiation. Well-known phenomena that belong to this category include irradiation growth, irradiation creep, and void swelling.

To understand irradiation damage processes, it is essential to understand the interaction between point defects and sinks. Basically, the interaction of a point defect with a sink results in a modification of the potential barriers to possible atomic jumps, subsequently affecting the migration of the point defect. In metallic crystalline materials, the main contribution to the interaction energy is due to the long-range elastic interaction between the strain field of the point defect and those of the

sink and the externally applied stress, if any. This interaction energy can be expressed by [1]

$$E(\underline{r}) = [-P_{ij} - \frac{1}{2}\alpha_{ijkl}\xi_{kl}(\underline{r})]\xi_{ij}(\underline{r}) \tag{1}$$

where

$$\xi_{ij}(\underline{r}) = e_{ij}(\underline{r}) + \varepsilon_{ij}(\underline{r}) \quad . \tag{2}$$

Repeated indices imply summation. A lower case Roman index may have a value of 1, 2 or 3, while a Greek index may have a value of 1 or 2 only. $e_{ij}(\underline{r})$ is the strain field of the sink, and $\varepsilon_{ij}(\underline{r})$ is the strain field due to an externally applied stress at the point defect position, $\underline{r}$. P_{ij} is the elastic dipole tensor of the point defect, so named because P_{ij} represents the magnitude and direction of the three mutually perpendicular force dipoles that, when placed at $\underline{r}$, would produce the same linear elastic strain field as the point defect. α_{ijkl} is the elastic polarizability of the point defect and describes the modification of the point-defect dipole tensor due to the applied stress.

The point-defect arrival rate at a sink must be calculated within a drift-diffusion theory. In most previous calculations, the continuum theory of drift-diffusion was employed and the diffusion tensor was assumed to be isotropic. With these assumptions, the point-defect drift-diffusion current is given by

$$\underline{j} = -D_o \nabla C(\underline{r},t) - \beta D_o C(\underline{r},t)\nabla E(\underline{r},t) \tag{3}$$

where D_o is the ideal diffusion coefficient, β is the reciprocal of the product of Boltzmann's constant and the absolute temperature, and $C(\underline{r},t)$ is the point-defect concentration.

Much useful information has been derived concerning point-defect migration into sinks that have a significant associated strain field, e.g. edge dislocations, using equation (3). In these calculations, $E(\underline{r})$ is replaced by $-p\Delta V$, where ΔV is the isotropic volume strain of the point defect, which interacts with the hydrostatic component, p, of the stress field of the sink. Since ΔV for an interstitial is greater than that for a vacancy, the current of interstitials into any sink with a positive value of p will be greater than the current of vacancies into the same sink, assuming equal supersaturation of both types of point defects. The sink is said to have a larger sink strength for interstitials than for vacancies, and is also said to be biased towards interstitials (sink strength and bias will be defined in Section 2). Sinks that are biased towards interstitials include vacancy loops, interstitial loops and straight edge dislocations, but not straight screw dislocations since the associated strain field is in pure shear (i.e. p=0) in this case. The existence of biased sinks is very important in the explanation of many irradiation deformation phenomena, such as void swelling, and irradiation creep and growth [2].

Furthermore, based on equation (3), application of a uniform external stress can affect the point-defect drift-diffusion through the cross term contained in the second term on the right hand side of equation (1). This effect causes the bias to depend on the relative orientation of the Burgers vector [3-5] and line direction [4] with respect to the external stress field, and gives rise to a stress-induced preferred absorption (SIPA) effect, which is a favoured mechanism to explain irradiation creep [2-6].

However, it has been pointed out that equation (3) is, in general, inadequate [7-10]. Through a microscopic derivation, Dederichs and Schroeder [10] showed that if the saddle-point configuration of the point defect is isotropic, then the form of equation (3) can be retained by replacing D_o with $D = D_o \exp[-\beta(E_s-E_g)]$ and E with E_g, where E_s is the drift potential when the point defect is in the saddle-point configuration and E_g is the corresponding quantity in the equilibrium configuration. All previous results can then be used by replacing E with E_s and C with $C \exp[-\beta(E_s-E_g)]$ [11,12]. However, the saddle-point configuration of point defects is not isotropic, in general. This has been verified for cubic metals by computer simulations [13-15]. The work necessary to modify the continuum theory to include the shape of the point defect in the saddle-point configuration is extensive but necessary; otherwise important effects may be overlooked, as the evidence presented below would suggest.

The effect of saddle-point anisotropy, also known as saddle-point shape effect (SAPSE), on the point-defect migration into an infinitesimal edge dislocation loop (IEDL) was studied by Woo [16]. It was found that, while both types of loops (vacancy and interstitial) had a bias for interstitials, the vacancy loop had a larger bias by a factor of approximately 5/3 in fcc copper and approximately 4/3 in bcc iron. Previously it was believed that the two types of loops had the same bias. This bias differential has important implications towards explaining the simultaneous growth of vacancy and interstitial loops in some materials [16].

As mentioned earlier, an isotropic point defect does not interact with the strain field of a screw dislocation. However, Bullough and Newman [17] pointed out that the shear field of an anisotropic point defect

will interact with the pure shear strain field of a screw dislocation. From this point of view, screw dislocations may be biased sinks and, if so, may be an important factor in irradiation damage calculations.

More evidence that SAPSE is an important effect can be found in the case of an externally applied stress. The effect of an externally applied stress on the bias of a straight edge dislocation was first considered by Heald and Speight [2] and Wolfer and Ashkin [6]. It was envisaged to be caused by a change in the point-defect/dislocation interaction due to the induced change in the dipole tensor by an external shear, represented by the second term in equation (1). As mentioned earlier, this is the basis of the SIPA mechanism often used to explain the phenomenon of irradiation creep [2-6]. It has been pointed out [7-10] that the non-equivalence of the jump directions in external fields due to the anisotropy of the saddle-point configurations could add to the stress effect on the bias. Woo [16] found that the bias change for an IEDL due to SAPSE had the same stress dependence as the usual SIPA effect, and named the resulting stress-induced preferred absorption effect SIPA-SAPSE to distinguish it from the usual SIPA effect which he called SIPA-I. The magnitude of the bias change due to SIPA-SAPSE for an IEDL was found to be more than an order of magnitude larger than that of the SIPA-I effect in fcc copper and bcc iron. The SIPA-SAPSE results appear to be in better agreement with experiment than the SIPA-I results [16].

Recently, Tomé et al. [18] numerically solved the drift-diffusion equations for point defects, including SAPSE*, in the strain field of a straight edge dislocation in a high-density dislocation lattice, and with an externally applied uniaxial stress. For fcc copper, they found that the dependence of the dislocation sink strength on the orientation of the uniaxial stress relative to the Burgers vector was small and negative, whereas the dependence on the orientation of the uniaxial stress relative to the line direction was much larger in magnitude and also negative. The usual SIPA theory predicts both coefficients to be positive, and the dependence of the orientation of the uniaxial stress with the Burgers vector to be larger. These results suggest that the shape of point defects in their saddle-point configuration may have an important consequence for irradiation damage studies.

However, being a numerical solution, the calculation of Tomé et al. may encounter the following difficulties. Firstly, numerical results are normally less physically transparent, especially in the case of the bias of a dislocation since it is a function of many variables. Secondly, numerical results are difficult to incorporate in rate-theory calculations of the macroscopic effects of irradiation deformation. Thirdly, numerical accuracy limits the approximate magnitude of the external applied elastic strain. Consequently, their calculation had to be performed using an incremental elastic strain step of 10^{-3}, which may be more than an order of

---

* Tomé et al. [18] claimed that their results contain effects beyond SAPSE, which came from the anisotropy of the equilibrium configuration. The author concurs with Dederichs and Schroeder [10] and maintains that the anisotropy of the equilibrium configuration does not lead to anisotropic diffusion in a cubic crystal, even in the presence of a small deviatoric applied stress.

magnitude larger than appropriate under normal conditions, where terms of order of ϵ^2 can be safely ignored. The non-linear stress dependence of their results is quite apparent. Fourthly, limitation of the size of the integration region makes it difficult to calculate cases where sink densities are more dilute.

The purpose of this thesis is to study analytically the biases of infinite straight edge and screw dislocations in the absence and presence of an externally applied stress including the full effect of the saddle-point anisotropy. The results are applied to fcc copper and bcc iron, and the implications of the results are discussed.

Chapter 2

FORMULATION

We now consider point-defect drift-diffusion in an applied strain field, $\xi_{k\ell}(\underset{\sim}{r})$, taking into account the anisotropy of the saddle-point configurations. From the microscopic derivation of Dederichs and Schroeder [10], this can be described in terms of the renormalized density $W(\underset{\sim}{r},t) = C(\underset{\sim}{r},t)\exp(\beta E_g)$ by the Lagrangian

$$L[W(\underset{\sim}{r},t)] = \int \frac{d^3\underset{\sim}{r}}{V} \left[D_{ij}(\underset{\sim}{r}) \frac{\partial W(\underset{\sim}{r},t)}{\partial r_i} \frac{\partial W(\underset{\sim}{r},t)}{\partial r_j} - K(\underset{\sim}{r})W(\underset{\sim}{r},t) \right] \tag{4}$$

where V is the integration volume, $K(\underset{\sim}{r})$ is the point-defect production rate, and $D_{ij}(\underset{\sim}{r})$ is the renormalized diffusion tensor given by *

$$D_{ij}(\underset{\sim}{r}) = \frac{1}{2} \sum_{\underset{\sim}{h}} h_i h_j \lambda^o_{eff}(\hat{\underset{\sim}{h}}) \exp[\beta \xi_{k\ell}(\underset{\sim}{r}) P^s_{k\ell}(\hat{\underset{\sim}{h}})] \tag{5}$$

where the summation is over all nearest-neighbour position vectors, $\underset{\sim}{h}$, to which a jump may occur. The superscript, s, in $P^s_{k\ell}(\hat{\underset{\sim}{h}})$ indicates that we are referring to the dipole tensor of the point defect in the saddle-point configuration. $P^s_{k\ell}(\hat{\underset{\sim}{h}})$ is defined in the perfect crystal, and therefore we are assuming that the applied strain does not perturb the dipole tensor. In so doing, we are neglecting the second term of equation (1) in the argument of the exponential in equation (5). This is to facilitate study of the intrinsic shape effect alone and not the stress-induced one. We further note that λ^o_{eff} in equation (5) is an effective [10] (i.e. averaged over different non-equivalent equilibrium configurations of the point defect) ideal jump frequency in the $\hat{\underset{\sim}{h}}$ direction, and $W(\underset{\sim}{r},t)$ in equation (4)

---

* The symbol $\hat{}$ in $\hat{\underset{\sim}{h}}$ denotes the unit vector in the direction of $\underset{\sim}{h}$. This symbol is used throughout the report with similar meaning.

refers to the total concentration of non-equivalent equilibrium configurations of the same defect [10]. We emphasize that, as a result of λ^{o}_{eff}, the possible jump directions are no longer those of only one particular equilibrium configuration, but are those of any one of the equivalent equilibrium configurations. The effect of an external applied stress on the equilibrium energies does not affect this situation [10]. Equations (4) and (5) hold regardless of the symmetry of the point defect, as long as we can neglect the dependence of $P^{s}_{k\ell}$ on the orientations of the point defect before and after the jump. In cases where we can drop the $\hat{h}_j$ dependence of λ^{o}_{eff}, we may write equation (5) as

$$\overset{\leftrightarrow}{D}_{ij}(\underset{\sim}{r}) = D_o \frac{3}{Z} \sum_{\hat{h}_j} \hat{h}_i \hat{h}_j \exp[\beta \xi_{k\ell} P^{s}_{k\ell}(\hat{h}_j)] \tag{6}$$

where Z is the coordination number and D_o is the ideal diffusion coefficient given by $D_o = \frac{Z}{6} h^2 \lambda^{o}_{eff}$. In non-cubic cases, the same assumption leads to an approximation where the anisotropy of the ideal jump frequency is averaged out. Within this approximation, D_o is replaced by the averaged ideal diffusion coefficient, D_o^{eff}, which is effectively what has been used in equation (3) in most previous calculations [19-22]. Although this may not be a good approximation in certain cases, the averaging allows the unmasking of the effect due to the anisotropy of the saddle-point configuration (from that due to the anisotropy of the ideal jump frequency or jump distance) of the point defect, which is of interest in the present investigation.

The extremum principle, when applied to equation (4), results in a boundary value problem which cannot be solved analytically. One further approximation is necessary to make the problem tractable. In this paper,

we consider the case of the infinite, straight edge or screw dislocation. Both dislocation types have translational symmetry along their line directions. Accordingly, we choose a cylindrical polar coordinate system with the line direction of the dislocation along the z-axis. We now approximate the renormalized density by a cylindrically symmetric ansatz, $W(\underset{\sim}{r}) \simeq n_o(r)$. Note that r now represents the cylindrical polar coordinate. This is similar to the spherical symmetrization procedure first introduced by Schroeder and Dettmann [12] and used successfully in other applications [22]. After making this approximation, the extremum principle for the Lagrangian gives the following one-dimensional, second-order differential equation:

$$\frac{1}{r}\frac{d}{dr}\left[r\overset{\leftrightarrow}{D}_{eff}(r)\frac{dn_o}{dr}\right] + K(r) = 0 \tag{7}$$

where

$$\overset{\leftrightarrow}{D}_{eff}(r) = \int_o^{2\pi} \frac{d\theta_r}{2\pi}\, \hat{r}_\mu \overset{\leftrightarrow}{D}_{\mu\nu}(\underset{\sim}{r})\hat{r}_\nu \quad . \tag{8}$$

$\hat{r}_\mu$ refers to the μth component of the unit vector along $\underset{\sim}{r}$ in cylindrical polar coordinates. Note that here, as elsewhere, Greek letter subscripts take only the values 1 and 2. Note also that equations (7) and (8) are inherently different from their counterparts resulting from the spherical symmetrization procedure in the case of the IEDL [16], thus requiring a separate derivation.

Replacing $\xi_{k\ell}(\underset{\sim}{r})P^s_{k\ell}(\hat{h})$ by $-E_s(\underset{\sim}{r},\hat{h})$ in equation (6) and substituting into equation (8), we obtain

$$\overset{\leftrightarrow}{D}_{eff}(r) = D_o^{eff}\frac{3}{Z}\sum_{\hat{h}} \int_o^{2\pi} \frac{d\theta_r}{2\pi}(\hat{r}\cdot\hat{h})^2 \exp[-\beta E_s(\underset{\sim}{r},\hat{h})] \tag{9}$$

where D_o^{eff} is the diffusion coefficient in the stress-free crystal. It is usually not a bad approximation to assume that the effective jump directions are isotropic and replace the summation by an integration. Then $\underset{\sim}{D}_{eff}(r)$ becomes

$$\underset{\sim}{D}_{eff}(r) = 3D_o^{eff} \int \frac{d\Omega_h}{4\pi} \int_o^{2\pi} \frac{d\theta_r}{2\pi} (\hat{\underset{\sim}{r}} \cdot \hat{\underset{\sim}{h}})^2 \exp[-\beta E_s(\underset{\sim}{r}, \hat{\underset{\sim}{h}})] \quad . \tag{10}$$

If we define

$$g(r) = 3 \int \frac{d\Omega_h}{4\pi} \int_o^{2\pi} \frac{d\theta_r}{2\pi} (\hat{\underset{\sim}{r}} \cdot \hat{\underset{\sim}{h}})^2 \exp[-\beta E_s(\underset{\sim}{r}, \hat{\underset{\sim}{h}})] \quad , \tag{11}$$

then equation (10) can be written as

$$\underset{\sim}{D}_{eff}(r) = D_o^{eff} g(r) \tag{12}$$

where g(r) can be interpreted as a scaled effective drift potential for the point defect.

The shape effect can now be considered. To allow focusing on it as much as possible, we make the simplifying assumption that K(r) = 0 in equation (7) and use the simplest set of boundary conditions, which is generally referred to as the Constant Boundary Concentration Method [23]. We imagine the dislocation to be surrounded by a cylindrical reservoir of radius, R, centred at the dislocation and maintained at a constant point-defect concentration, $\bar{C}$. The concentration at the dislocation core is assumed to be the thermal equilibrium concentration, so that the renormalized concentration then is given by

$$n_o(r_o) = C^e \tag{13}$$

where C^e is the thermal equilibrium concentration far from a dislocation. r_o is the radius from the straight dislocation at which a point defect will find it difficult to leave the dislocation by thermal motion alone. Once inside r_o, the point defect is assumed to be absorbed by the dislocation.

Thus, r_o is termed the capture radius. With these assumptions, the current of point defects through a unit volume can be written as

$$I = \frac{D_o^{eff}}{\Omega}(\bar{C} - C^e)k^2 \tag{14}$$

where Ω is the atomic volume, and k^2 is called the sink strength and is a measure of the ability of a sink to absorb point defects. The derivation of the expression for the sink strength can be found in Appendix A, with the result expressed in terms of ζ, the sink strength per unit dislocation line length:

$$\zeta \equiv k^2/\rho = 2\pi\left[\int_{r_o}^{R} \frac{dt}{tg(t)}\right]^{-1} \tag{15}$$

where

$$R = (\pi\rho)^{-1/2} \tag{16}$$

and ρ is the dislocation line density. Another quantity of interest is the bias, B, which describes whether a sink has a larger sink strength for an interstitial or a vacancy:

$$B = \frac{\zeta_i - \zeta_v}{\zeta_i} \quad . \tag{17}$$

Thus, a sink with a negative bias will have a larger sink strength for vacancies whereas a sink with a positive bias will have a larger sink strength for interstitials. As explained in the introduction, the bias of a dislocation has important consequences for the macroscopic effects of irradiation damage in metals.

Finally, for the evaluation of g(r), we use the identity

$$P^s_{ij}(\hat{h}) = P p_n \, e_i^{(n)} e_j^{(n)} \tag{18}$$

where $P = \frac{1}{3} \mathrm{Tr}(P^s_{ij})$, p_n is a normalized eigenvalue so that Pp_n is the nth eigenvalue of $P^s_{ij}(\hat{\underset{\sim}{h}})$, and $\underset{\sim}{e}^{(n)}$ is the nth normalized eigenvector of $P^s_{ij}(\hat{\underset{\sim}{h}})$. Note that

$$\sum_n p_n = 3 \quad . \tag{19}$$

Thus,

$$E_s(\underset{\sim}{r},\hat{\underset{\sim}{h}}) = -Pp_n \, \xi_{ij}(\underset{\sim}{r}) e_i^{(n)} e_j^{(n)} \quad . \tag{20}$$

Chapter 3

THE BIAS OF STRAIGHT DISLOCATIONS WITH NO EXTERNAL APPLIED STRESS

3.1 CALCULATION OF g(r) FOR AN EDGE DISLOCATION

The strain field of an infinite straight edge dislocation, with the line direction along the z-axis and the Burgers vector along the x-axis, is given by [24]

$$e_{11} = -\frac{\kappa}{r}[2(1-\nu)\hat{y}+\hat{y}(\hat{x}^2-\hat{y}^2)],$$

$$e_{22} = \frac{\kappa}{r}[2\nu\hat{y}+\hat{y}(\hat{x}^2-\hat{y}^2)], \tag{21}$$

$$e_{12} = \frac{\kappa}{r}\hat{x}(\hat{x}^2-\hat{y}^2) = e_{21},$$

with

$$\kappa = \frac{b}{4\pi(1-\nu)}$$

where b is the magnitude of the Burgers vector, ν is Poisson's ratio, and $\hat{x}$ and $\hat{y}$ are given by

$$\hat{x} = \hat{r}_1 = \cos\theta_r,$$
$$\hat{y} = \hat{r}_2 = \sin\theta_r \quad . \tag{22}$$

where θ_r is the polar angle. All other elements of e_{ij} are zero. It is convenient to separate e_{ij} into its isotropic and deviatoric components. Thus,

$$e_{ij} \equiv \frac{1}{3}\delta_{ij}e_{kk}+f_{ij}$$

where f_{ij} is the deviatoric component, and δ_{ij} is the usual Kronecker delta function. Note that

$$e_{kk} = -2(1-2\nu)\frac{\kappa}{r}\hat{y} \tag{23}$$

and

$$f_{kk} = 0 \quad . \tag{24}$$

Therefore, in the absence of an externally applied stress,

$$E_s = -Pe_{kk} - Pp_n f_{ij} e_i^{(n)} e_j^{(n)} \tag{25}$$

and

$$g(r) = 3 \sum_{m=0}^{\infty} \frac{(\beta P)^m}{m!} \int_0^{2\pi} \frac{d\theta_r}{2\pi} \int \frac{d\Omega_h}{4\pi} (\hat{r}\cdot\hat{h})^2 \exp(\beta P e_{kk}) (p_n f_{ij} e_i^{(n)} e_j^{(n)})^m \quad . \tag{26}$$

In order to integrate over all $\hat{h}$, we make the assumption that $\hat{h}$ lies along the first principal direction of the point-defect dipole tensor. This is valid in most cases, since $\hat{h}$ is usually in a direction of high symmetry of the point-defect saddle-point configuration. Therefore,

$$\hat{h} = e^{(1)} \quad . \tag{27}$$

Additionally, we must relate $e^{(2)}$ and $e^{(3)}$ to $\hat{h}$.

In Appendix B, we show that

$$e_i^{(n)} e_j^{(n)} = \frac{1}{2}[\hat{h}_i \hat{h}_j (3\delta_{nl} - 1) + \delta_{ij}(1 - \delta_{nl})] \quad . \tag{28}$$

(no implied summation)

Substitution into equation (26) gives

$$g(r) = \frac{3}{2\pi} \int_0^{2\pi} \hat{r}_\mu \hat{r}_\nu \exp(\beta P e_{kk}) \gamma(\mu,\nu) d\theta_r$$

$$+ \frac{3}{2\pi} \sum_{m=1}^{\infty} \frac{1}{m!} [\frac{3}{2} \beta P (p_1 - 1)]^m \int_0^{2\pi} \hat{r}_\mu \hat{r}_\nu \exp(\beta P e_{kk}) \tag{29}$$

$$\cdot f_{i_1 j_1} f_{i_2 j_2} \cdots f_{i_m j_m} \gamma(\mu,\nu,i_1,j_1,\cdots i_m,j_m) d\theta_r$$

where

$$\gamma(\mu,\nu,i_1,j_1 \cdots i_m,j_m) = \int \frac{d\Omega_h}{4\pi} \hat{h}_\mu \hat{h}_\nu \hat{h}_{i_1} \hat{h}_{j_1} \cdots \hat{h}_{i_m} \hat{h}_{j_m} \, . \tag{30}$$

The evaluation of equation (29) is carried out in Appendix C with the result that

$$g(r) = 1 + F^E (\frac{b}{r})^2 + 0(r^{-4}) \tag{31}$$

where F^E is given by

$$F^E = \frac{\beta^2 P^2 (1-2\nu)^2}{16\pi^2(1-\nu)^2}\left[1 + \frac{1}{5}(p_1-1) + \frac{1}{140}\left\{5 + \frac{27}{(1-2\nu)^2}\right\}(p_1-1)^2\right]. \qquad (32)$$

The first term in the square bracket of equation (32) represents the contribution to the drift potential due to the interaction between the hydrostatic components of the strain fields of the point defect and the dislocation, and is the origin of the so-called "size effect" in the usual rate theory of irradiation damage [1]. The third term represents the contribution due to the interaction between the deviatoric component of the displacement field of the point defect and the shear component of the strain field of the dislocation. This term vanishes in the case where the point defect is isotropic, i.e. when $p_1=1$ (we assume $p_2 = p_3$). The second term arises as a cross term between the two terms in the definition of E_s (equation (25)) caused by the non-linearity of the exponential in the definition of the effective drift potential in equation (11). The last two terms represent the effect of the saddle-point anisotropy on point-defect drift-diffusion in the field of a straight edge dislocation. It will be shown in Section 5 that, in the stress-free case, this effect only changes the sink strength and bias of the edge dislocation by a small amount. This change is an increase in most cases, except when p_1 lies in the range $0.89<p_1<1$, as can be shown from equation (32).

3.2 CALCULATION OF g(r) FOR A SCREW DISLOCATION

The strain field of an infinite straight screw dislocation with the line direction along the z-axis is given by [24]

$$e_{13} = -\frac{b}{4\pi r}\hat{y} = e_{31}$$

and (33)

$$e_{23} = \frac{b}{4\pi r}\hat{x} = e_{32}$$

where the symbols have the same meaning as in the straight edge dislocation case. All other elements of e_{ij} are zero. Note that

$$e_{kk} = 0 \tag{34}$$

and so separation of e_{ij} into isotropic and deviatoric components is unnecessary. The interaction energy can be conveniently written as

$$E_s(\underset{\sim}{r},\hat{\underset{\sim}{b}}) = -\frac{b}{2\pi r}P p_n G_{\mu\nu}\hat{r}_\mu e_\nu^{(n)} e_3^{(n)} \tag{35}$$

where

$$G = \begin{pmatrix} 0 & 1 \\ -1 & 0 \end{pmatrix} \quad . \tag{36}$$

The G tensor has some useful properties which are listed below:

$$G_{\mu\nu}\hat{r}_\mu\hat{r}_\nu = 0$$

and (37)

$$G_{\mu\kappa}G_{\nu\kappa} = \delta_{\mu\nu} \quad .$$

Substituting equation (28) into equation (35), gives

$$E_s = -\frac{b}{4\pi r}P(p_1-1)G_{\mu\nu}\hat{r}_\mu\hat{h}_\nu\hat{h}_3 \quad . \tag{38}$$

We note that, for an isotropic point defect (p_n=1, n=1,2,3), $E_s = 0$, as mentioned in the Introduction. Continuing as for the straight edge dislocation, we find, for the straight screw dislocation (see Appendix D)

$$\begin{aligned} g(r) &= 6\sum_{m=0}^{\infty}\frac{[(2m+1)!!]^2}{(2m+1)(4m+3)!}A^{2m}\left(\frac{b}{r}\right)^{2m} \\ &= 1+F^S\left(\frac{b}{r}\right)^2+0(r^{-4}) \end{aligned} \tag{39}$$

where

$$F^S = \frac{9\beta^2P^2}{1120\pi^2}(p_1-1)^2 \tag{40a}$$

and

$$A = \frac{3\beta P}{2\pi}(p_1-1) \quad . \tag{40b}$$

Equations (39) and (40) clearly show that the contribution to the drift potential in the case of a screw dislocation comes only from the interaction between the shear components of the fields. Drift due to a "size effect" interaction is completely absent (cf. equation (32)). It can be seen immediately that the drift potential vanishes for an isotropic defect, where $p_1=1$. As a consequence of the saddle-point anisotropy, screw dislocations are generally biased sinks. However, unlike edge dislocations, which are usually biased towards interstitials, screw dislocations can be biased towards vacancies in cases where the "degree" of anisotropy of vacancies [determined by $(p_1-1)^2$] is much larger than that of interstitials. This is because, for edge dislocations, the drift potential is dominated by the "size effect" interaction, which is larger for interstitials because of their larger hydrostatic strain field. The analogous hydrostatic strain field does not contribute to the interaction of the point defects and the screw dislocation. This bias of a screw dislocation is entirely an effect of the saddle-point anisotropy and may have important consequences for the interpretation of irradiation damage experiments.

3.3 THE SINK STRENGTH AND BIAS

Having derived expressions for g(r) for both types of dislocations, we can now evaluate the sink strengths and biases from equation (15). From equations (31) and (39) we can write

$$g(r) \simeq 1 + F\left(\frac{b}{r}\right)^2 \quad . \tag{41}$$

For simplicity, we have dropped the superscripts E and S that indicate the type of dislocation. The sink strength per unit line length can now be evaluated from equation (15):

$$\zeta = \frac{4\pi}{\ln(R^2+Fb^2)-\ln(r_o^2+Fb^2)} \tag{42}$$

and the bias can be written as

$$B = 1-\left\{\frac{\ln(R^2+F_v b^2)-\ln(r_o^{\,2}+F_v b^2)}{\ln(R^2+F_i b^2)-\ln(r_o^{\,2}+F_i b^2)}\right\}^{-1} \tag{43}$$

where the subscripts i and v refer to interstitial and vacancy respectively.

If we put

$$P = K\Delta V = \frac{2}{3}\frac{1+\nu}{1-2\nu}\mu V\varepsilon_o$$

where K is the bulk compressibility, μ the shear modulus, V the volume and ε_o the relaxation strain of the point defect, then assuming $R^2 \gg Fb^2 \gg r_o^{\,2}$, it can be shown that, for an isotropic point defect, equation (42) reduces to

$$\zeta \simeq \frac{2\pi}{\ln(3\pi R/\beta\mu V\varepsilon_o b)}$$

which can be compared with the one derived by Heald and Speight [2,4] for similar conditions:

$$\zeta \simeq \frac{2\pi}{\ln(2.3\pi R/\beta\mu V\varepsilon_o b)} \quad .$$

A discussion of the validity of neglecting $O(r^{-4})$ in g(r) in equation (41) and of the accuracy of equation (42) is given in Appendix G.

Chapter 4

THE EFFECTS OF AN EXTERNALLY APPLIED STRESS

If $\epsilon_{ij}(\underset{\sim}{r})$ of equation (2) is caused by a uniform externally applied stress, then we may use the identity

$$\epsilon_{ij} = \epsilon s_m t_i^{(m)} t_j^{(m)} \tag{44}$$

where $\epsilon = \frac{1}{3}\mathrm{Tr}(\epsilon_{ij})$, s_m is a normalized eigenvalue so that ϵs_m is the m-th eigenvalue of ϵ_{ij}, and $\underset{\sim}{t}^{(m)}$ is the m-th normalized eigenvector of ϵ_{ij}. Again, we have

$$\sum_m s_m = 3 \quad . \tag{45}$$

Thus the contribution to E_s due to the externally applied stress can be written as

$$E_s^e(\hat{\underset{\sim}{h}}) = - P\epsilon p_n s_m t_i^{(m)} t_j^{(m)} e_i^{(n)} e_j^{(n)} \quad . \tag{46}$$

Denoting $E_s(\underset{\sim}{r},\underset{\sim}{h})$ in equation (20) by $E_s^i(\underset{\sim}{r},\hat{\underset{\sim}{h}})$, we have

$$E_s(\underset{\sim}{r},\hat{\underset{\sim}{h}}) = E_s^i(\underset{\sim}{r},\hat{\underset{\sim}{h}}) + E_s^e(\hat{\underset{\sim}{h}}) \quad . \tag{47}$$

ζ can be expanded in a McLaurin series in terms of ϵ. We only consider the physically important range in which the external stress satisfies $E_s^e << E_s^i$. In this range, we may neglect terms of $0(\epsilon^2)$ and higher. Therefore

$$\zeta(\epsilon) \simeq \zeta(0)(1+\frac{\Delta\zeta}{\zeta}) \tag{48}$$

where

$$\frac{\Delta\zeta}{\zeta} = \frac{1}{\zeta}\frac{d\zeta}{d\epsilon}\Big|_{\epsilon=0} \epsilon \quad . \tag{49}$$

Then, from equation (15)

$$\frac{\Delta\zeta}{\zeta} = \epsilon \int_{r_o}^{R} \frac{g'(t)dt}{t[g(t)]^2} \Big/ \int_{r_o}^{R} \frac{dt}{tg(t)} \tag{50}$$

where

$$g'(t) = \frac{dg(t)}{d\varepsilon}\Big|_{\varepsilon=0} \quad . \tag{51}$$

The change of the bias due to the externally applied stress is, from equation (17),

$$\Delta B = \frac{\zeta_v}{\zeta_i}\left(\frac{\Delta\zeta_i}{\zeta_i} - \frac{\Delta\zeta_v}{\zeta_v}\right) \quad . \tag{52}$$

Substituting equation (28) into equation (46), we obtain

$$E_s^e(\hat{\underset{\sim}{h}}) = -3P\varepsilon - \frac{3}{2}P\varepsilon(p_1-1)(s_n t_i^{(n)} t_j^{(n)} \hat{h}_i \hat{h}_j - 1) \quad . \tag{53}$$

We observe that the first term of equation (53) is independent of $\hat{\underset{\sim}{h}}, \underset{\sim}{r}$, and p_n and can therefore be taken outside the double integral of equation (12). In fact, we can define

$$D_o^{eff}(\varepsilon) = D_o^{eff} \exp(3\beta P\varepsilon) \quad . \tag{54}$$

$D_o^{eff}(\varepsilon)$ represents the change of the ideal diffusion coefficient under a hydrostatic pressure. Thus equations (12) and (11) can be rewritten explicitly in terms of the internal applied stress as

$$D_{eff}(r,\varepsilon) = D_o^{eff}(\varepsilon) g(r,\varepsilon) \tag{55}$$

and

$$g(r,\varepsilon) = 3\int \frac{d\Omega_h}{4\pi} \int_0^{2\pi} \frac{d\theta_r}{2\pi} (\hat{\underset{\sim}{r}} \cdot \hat{\underset{\sim}{h}})^2 \exp[-\beta E_s^i(\underset{\sim}{r}, \hat{\underset{\sim}{h}}) - \beta E_s^{ed}(\hat{\underset{\sim}{h}}, \varepsilon)] \tag{56}$$

where

$$E_s^{ed}(\hat{\underset{\sim}{h}}, \varepsilon) = -\frac{3}{2}\beta\varepsilon(p_1-1)(s_n t_i^{(n)} t_j^{(n)} \hat{h}_i \hat{h}_j - 1) \quad . \tag{57}$$

Note that $E_s^{ed}(\hat{\underset{\sim}{h}}, \varepsilon)$ in equation (57) vanishes for a pure hydrostatic applied stress ($s_n=1$, $n=1,2,3$). We can now evaluate $g'(r)$ and obtain

$$g'(r) = \frac{9}{2}\beta P(p_1-1) \int \frac{d\Omega_h}{4\pi} \int_0^{2\pi} \frac{d\theta_r}{2\pi} (\hat{\underset{\sim}{r}} \cdot \hat{\underset{\sim}{h}})^2 (s_n t_i^{(n)} t_j^{(n)} \hat{h}_i \hat{h}_j - 1) \exp[-\beta E_s^i(\underset{\sim}{r}, \hat{\underset{\sim}{h}})] . \tag{58}$$

Note that for an isotropic point defect (p_n=1, n=1,2,3), g'(r) is zero. Thus, the change in bias that we will calculate is strictly due to the anisotropy of the saddle-point configuration of the point defect. The details of the evaluation of equation (58) for the edge dislocation are presented in Appendix E with the result that

$$g'(r) = \frac{3}{10}\beta P(p_1-1)[H^E_\beta \frac{b^2}{r^2}(1-s_n\cos^2\beta_n)+(1+H^E_\lambda \frac{b^2}{r^2})(1-s_n\cos^2\lambda_n)] \qquad (59)$$

where β_n is the angle between the Burgers vector of the edge dislocation and the nth principal direction of the externally applied stress, and λ_n is the corresponding angle for the line direction of the edge dislocation. H^E_β and H^E_λ are given by

$$H^E_\beta = \frac{\beta^2P^2}{112(1-\nu)^2\pi^2}[7(1-2\nu)^2-(7-10\nu-8\nu^2)(p_1-1)-(2-2\nu-\nu^2)(p_1-1)^2] \qquad (60)$$

and

$$H^E_\lambda = \frac{\beta^2P^2}{224(1-\nu)^2\pi^2}[21(1-2\nu)^2+(3-30\nu+48\nu^2)(p_1-1)+3(1+\nu^2)(p_1-1)^2]. \qquad (61)$$

In equation (59), we are neglecting terms of $O(r^{-4})$ and higher. Using the same approximation for the screw dislocation (see Appendix F)

$$\begin{aligned} g'(r) &= 36\beta P(p_1-1)\sum_{m=0}^{\infty}\frac{(1-m^2)[(2m+1)!!]^2}{(2m+1)(4m+5)!}A^{2m}(\frac{b}{r})^{2m}(1-s_n\cos^2\lambda_n) \\ &\simeq \frac{3}{10}\beta P(p_1-1)(1-s_n\cos^2\lambda_n) \end{aligned} \qquad (62)$$

where A is given by equation (40b).

If we separate the isotropic and deviatoric components, equation (48) can be rewritten as

$$\zeta(\epsilon_{k\ell}) = \zeta(0)[1+(\frac{\Delta\zeta}{\zeta})_{iso}+(\frac{\Delta\zeta}{\zeta})_\beta+(\frac{\Delta\zeta}{\zeta})_\lambda] \qquad (63)$$

where the $(\frac{\Delta\zeta}{\zeta})$'s are evaluated using equation (50) with

$$g'_{iso}(r) = g'_{\beta o}(r)+g'_{\lambda o}(r) \tag{64}$$

and

$$g'_{\mu}(r) = - g'_{\mu o}(r)s_n\cos^2\mu_n \quad , \quad \text{for } \mu = \beta \text{ or } \lambda \tag{65}$$

where

$$g'_{\beta o}(r) = \frac{3}{10}\beta P(p_1-1)H_\beta \frac{b^2}{r^2}$$

and (66)

$$g'_{\lambda o}(r) = \frac{3}{10}\beta P(p_1-1)(1+H_\lambda \frac{b^2}{r^2}) \quad .$$

The H values for the edge dislocations are given by equations (60) and (61). Those for the screw dislocations are both zero.

The isotropic component arises from the point-defect size effect interaction with the strain field of the external stress (equation (54)), plus the cross term arising from shape effect interaction with the shear strain fields of the straight dislocation and the size effect interaction with the isotropic component of the externally applied stress. It is independent of the stress orientation with respect to the Burgers vector and the line direction of the dislocation, and therefore does not cause preferred absorption of point defects. The deviatoric components, on the other hand, arises from the shape effect interaction with the combined strain fields of the straight dislocation and the deviatoric component of the external stress. It depends on the relative orientation of the Burgers vector and the line direction with respect to the externally applied stress direction, and therefore causes preferred absorption of point defects. We note that equation (63) guarantees that $\zeta(\varepsilon_{k\ell}) = \zeta(0)$ if $\varepsilon_{k\ell}$ has no devi-

atoric component. The effect of the hydrostatic component of $\varepsilon_{k\ell}$ has already been separated out and incorporated into the "ideal" diffusion coefficient.

If σ is the trace of the external applied stress tensor σ_{ij}, and u_n a normalized eigenvalue so that σu_n is the nth eigenvalue of σ_{ij} (see equation 44), we have the following relationship between the strain and the stress

$$\varepsilon = \frac{(1-2\nu)}{(2+2\nu)} \frac{\sigma}{3\mu} \tag{67}$$

and

$$s_n = \frac{(1+\nu)}{(1-2\nu)} u_n - \frac{3\nu}{(1-2\nu)} \tag{68}$$

where μ is the shear modulus. We note that the eigenvectors of σ_{ij} are the same as those of ε_{ij}. Using equations (48) and (63), the sink strength in the presence of σ_{ij} is given by

$$\zeta(\sigma_{ij}) = \zeta(0)\left[1+\tfrac{1}{2}\beta P\frac{\sigma}{\mu}\left\{\mathscr{A}^{\lambda}(1-u_n\cos^2\lambda_n)+\mathscr{A}^{\beta}(1-u_n\cos^2\beta_n)\right\}\right] \tag{69}$$

where

$$\mathscr{A}^{\lambda} = \frac{(p_1-1)}{10}\left[1+\frac{\zeta(0)}{4\pi}(H_{\lambda}-F)\frac{b^2\,(R^2-r_o^2)}{(R^2+Fb^2)(r_o^2+Fb^2)}\right] \tag{70}$$

and

$$\mathscr{A}^{\beta} = \frac{(p_1-1)}{10}\frac{\zeta(0)}{4\pi}H_{\beta}\frac{b^2\,(R^2-r_o^2)}{(R^2+Fb^2)\,(r_o^2+Fb^2)} \quad . \tag{71}$$

Here, the subscripts and superscripts denoting dislocation and point-defect types are dropped to simplify the notation.

The change in the corresponding bias by the σ_{ij} is then given by

$$\Delta B = (1-B)\frac{\sigma}{\mu}\left[\Delta T_{\lambda}(1-u_n\cos^2\lambda_n)+\Delta T_{\beta}(1-u_n\cos^2\beta_n)\right] \tag{72}$$

and

$$\Delta T_{\mu} = \frac{1}{2}\beta(P_i \mathscr{A}_i^{\mu} - P_v \mathscr{A}_v^{\mu}) \qquad \mu = \beta \text{ or } \lambda \quad . \qquad (73)$$

It is immediately obvious from equations (72) and (73) that the application of an external stress changes the bias of straight dislocations (both screw and edge) as a consequence of the saddle-point anisotropy. The resulting bias change varies as a function of the dislocation orientation with respect to the principal directions of the external stress. As a result, the biases of some dislocations would be raised while those of others, that are differently oriented, would be lowered. This would cause a stress-induced preferred absorption of point defects at the dislocations, in the same way as the usual SIPA mechanism for irradiation creep does [2-6]. Of course, it should be remembered that the usual SIPA is a consequence of the stress-induced anisotropy of the point-defect dipole tensor, whereas in the present work, the preferred absorption is caused by the intrinsic anisotropy of the point-defect dipole tensor. To highlight the difference between the SIPA effects arising from the two different origins, we have chosen to call the usual SIPA arising from the second-order inhomogeneity effect SIPA-I, and the SIPA we consider in this work SIPA-SAPSE, as mentioned in the Introduction. At this point, we must emphasize that although SIPA-SAPSE and SIPA-I have different origins, they are not mutually exclusive. In fact they should occur simultaneously. When the intrinsic anisotropy of the point-defect saddle point is small and the elastic polarizability of the point defect at the saddle point is large, one would expect SIPA-I to dominate over SIPA-SAPSE. Otherwise, the opposite would be expected. We note that a classical example used for SIPA is the split dumbbell interstitial [3], which deforms significantly under the action of a shear stress, i.e. it is said to be very soft in shear. However,

although much experimental evidence suggests that the equilibrium interstitial configuration in many cubic metals is consistent with the dumbbell picture, it is not obvious that this can be generalized to the saddle-point configuration.

The behaviour of SIPA-SAPSE can be studied most readily by comparison with SIPA-I. The change in the sink strength of an edge dislocation due to the second-order inhomogeneity effect, as a function of the dislocation orientation, has been derived [3,4] using the linear elasticity theory. Using this result, and assuming that the interstitial is soft in shear while the vacancy shear modulus is unaffected by the external stress, the corresponding bias change of the edge dislocation can be cast in the same form as equations (72) and (73), as follows:

$$\Delta W^I = (1-B)\frac{\sigma}{\mu}[\Delta W_\lambda(1-u_n\cos^2\lambda_n)+\Delta W_\beta(1-u_n\cos^2\beta_n)] \tag{74}$$

where

$$\Delta W_\beta = -\frac{\zeta(0)}{\varepsilon_i^o}\frac{5\Delta\mu_i}{30(1-\nu)+4(4-5\nu)\Delta\mu_i} \tag{75}$$

and

$$\Delta W_\lambda = \nu\Delta W_\beta \quad . \tag{76}$$

Here ε_i^o is the relaxation strain of the interstitial in the absence of the external applied stress, and $\mu_i(1+\Delta\mu_i)$ is its shear modulus. Note that for a uniaxial external stress $u_\alpha = (3,0,0)$. Comparing equations (74) and (72), we note this remarkable similarity, with one governing the bias change upon the application of an external stress due to SIPA-I and the other governing that due to SIPA-SAPSE, respectively.

Although SIPA-I and SIPA-SAPSE are indistinguishable with respect to the linear stress dependence and the stress-orientation dependence of the resulting irradiation creep, the two mechanisms do differ in many respects. Perhaps the most important one is the relative significance of the line direction dependence and the Burgers vector dependence. For SIPA-I, the line direction dependence is about 1/3 of the Burgers vector dependence (see equation (76)). On the other hand, for SIPA-SAPSE, the line direction dependence is roughly 10 times larger than the Burgers vector dependence, as can be shown from a rough estimate of the ratio of $\mathscr{A}^{\lambda}/\mathscr{A}^{\beta}$ in equations (70) and (71). This large line direction dependence in the case of SAPSE is not related to the dislocation strain field and is solely a consequence of the external stress-induced anisotropy of the ideal diffusion tensor and the translational symmetry of the dislocation line. This symmetry dictates that all point-defect currents must flow in a plane normal to the dislocation line. A uniaxial tensile stress applied along the line direction will cause the material to elongate in the line direction and contract in the direction of the defect-current flow. An M-type point defect [16], which is elongated at the saddle point along the jump direction, would therefore encounter a higher energy barrier during its jump along the flow line than in the absence of the applied stress. On the other hand, an F-type point defect [16], which is flattened at the saddle point along the jump direction, would encounter a lower energy barrier than in the absence of the applied stress. Consequently, the applied stress lowers the sink strength of the dislocation for M-type defects and increases that for F-type defects. Thus, from equation (70), it can be seen that most of the contribution to $\mathscr{A}^{\lambda}$ comes from the first term in the square bracket. The second term contributes about 10%. That the first term is not related to the strain field can be readily seen by putting b=0, whereupon the second term vanishes. Note that $\mathscr{A}^{\beta}$ vanishes in this case

also. This shows that the second term of $\mathcal{I}^{\lambda}$ and the entire $\mathcal{I}^{\beta}$ are a consequence of the dislocation strain field, while the first term is related to the symmetry effect described in the foregoing discussion.

In the case of an edge dislocation loop, this line direction dependence translates into a Burgers vector direction dependence. It has been shown [25] that a finite edge dislocation loop may be approximated by averaging the line direction of an edge dislocation in a plane to which the Burgers vector is normal. In this approximation, the sink strength and bias of the loop are given by replacing $\cos^2\lambda_n$ by the average value [25] $\cos^2\lambda_n = 1/2(1-\cos^2\beta_n)$ in equations (69) and (72). It will be shown in the next section that this yields results consistent with those from a separate calculation for the infinitestimal edge dislocation loop [16].

The second difference between SIPA-I and SIPA-SAPSE is the temperature dependence. SIPA-SAPSE is inversely proportional to the absolute temperature explicitly, while SIPA-I is not explicitly temperature dependent. Any temperature dependence is through the temperature dependence of the sink strength, $\zeta(0)$. However, it is not experimentally easy to separate the temperature dependence of other effects such as thermal emission of vacancies from a sink, or bulk recombination.

The third difference is the dependence on the point-defect size. SIPA-SAPSE is directly proportional to the point-defect size through P, whereas SIPA-I is inversely proportional to the point-defect size. From computer simulation studies, the relaxation strain of copper is smaller than that of iron. Comparing the SIPA effect in copper and iron may provide an opportunity for experimental differentiation between these two mechanisms.

Chapter 5

APPLICATION TO FCC COPPER AND BCC IRON

The saddle-point dipole tensors for a vacancy and the <100> dumbbell interstitial have been calculated by computer simulation for both copper [13,14] and iron [14,15]. For copper, three sets of parameters are listed in Table 1 corresponding to different interatomic potentials of the modified Morse type [13,14]. For iron, one set of parameters is listed in Table 2, corresponding to a Johnson potential [14,15]. The sink strengths, per unit line length of an edge dislocation for anisotropic vacancies and interstitials in copper and iron at 500 K, are plotted against dislocation density in Figures 1 and 2. For comparison, the sink strengths for isotropic point defects are also plotted. In all cases, the interaction between the shear fields due to the shape anisotropy increases the sink strengths by a small amount. The case for the screw dislocations is similar. However, according to equation (32), the anisotropy can reduce the sink strength of an edge dislocation if p_1 lies in the narrow range $0.89<p_1<1$ (assuming $\nu=1/3$). In Figure 3, biases for both types of dislocation in copper have been plotted versus dislocation line density. The results show satisfactory consistency for the three different interatomic potentials. The screw dislocation has a slight bias for vacancies. This indicates that vacancies are more attracted to areas of shear strain than are <100> dumbbells. However, this bias is very small and may be insignificant in the presence of other sinks. On the other hand, the edge dislocation has a large bias for the <100> dumbbell. Therefore, in the presence of edge dislocations, more interstitials than vacancies will annihilate at the dislocation, leaving an excess of vacancies in the material. Voids, which are usually assumed to be neutral sinks, can grow under these conditions

TABLE 1

PARAMETERS FOR VACANCIES AND INTERSTITIALS IN THE SADDLE-POINT CONFIGURATION FOR FCC COPPER, OBTAINED BY COMPUTER SIMULATION

Defect	Potential	$Tr[P_{ij}]$ (eV)	P_1	P_2	P_3	$\underset{\sim}{e}^{(1)}=\hat{\underset{\sim}{h}}$	$\underset{\sim}{e}^{(2)}$	$\underset{\sim}{e}^{(3)}$	Reference
Vacancy Migration	M0	5.61	-0.73	0.21	3.52	$\begin{pmatrix}1\\1\\0\end{pmatrix}$	$\begin{pmatrix}1\\-1\\0\end{pmatrix}$	$\begin{pmatrix}0\\0\\1\end{pmatrix}$	14
<100> Interstitial Migration	M0	68.9	1.10	0.87	1.03	$\begin{pmatrix}1\\0\\1\end{pmatrix}$	$\begin{pmatrix}1\\0\\-1\end{pmatrix}$	$\begin{pmatrix}0\\1\\0\end{pmatrix}$	14
Vacancy Migration	M1	3.4	-1.13	0	4.13	$\begin{pmatrix}1\\1\\0\end{pmatrix}$	$\begin{pmatrix}1\\-1\\0\end{pmatrix}$	$\begin{pmatrix}0\\0\\1\end{pmatrix}$	13
<100> Interstitial Migration	M1	45.6	1.14	0.83	1.03	$\begin{pmatrix}1\\0\\1\end{pmatrix}$	$\begin{pmatrix}1\\0\\-1\end{pmatrix}$	$\begin{pmatrix}0\\1\\0\end{pmatrix}$	13
Vacancy Migration	MM	4.67	-1.01	0.31	3.70	$\begin{pmatrix}1\\1\\0\end{pmatrix}$	$\begin{pmatrix}1\\-1\\0\end{pmatrix}$	$\begin{pmatrix}0\\0\\1\end{pmatrix}$	14
<100> Interstitial Migration	MM	45.3	1.17	0.78	1.05	$\begin{pmatrix}1\\0\\1\end{pmatrix}$	$\begin{pmatrix}1\\0\\-1\end{pmatrix}$	$\begin{pmatrix}0\\1\\0\end{pmatrix}$	14

TABLE 2

PARAMETERS FOR VACANCIES AND INTERSTITIALS IN THE SADDLE-POINT CONFIGURATION FOR BCC IRON, OBTAINED BY COMPUTER SIMULATION

Defect	Potential	$Tr[P_{ij}]$ (eV)	p_1	p_2	p_3	$\underset{\sim}{e}^{(1)}=\hat{\underset{\sim}{h}}$	$\underset{\sim}{e}^{(2)}$	$\underset{\sim}{e}^{(3)}$	Reference
Vacancy Migration	Johnson	-2.82	2.73	0.135	0.135	$\begin{pmatrix}1\\1\\1\end{pmatrix}$	$\begin{pmatrix}1\\-1\\0\end{pmatrix}$	$\begin{pmatrix}1\\1\\-2\end{pmatrix}$	15
<100> Interstitial Migration	Johnson	63.1	1.50	0.89	0.61	$\begin{pmatrix}1\\1.05\\1\end{pmatrix}$	$\begin{pmatrix}1\\0\\-1\end{pmatrix}$	$\begin{pmatrix}1\\-1.90\\1\end{pmatrix}$	14

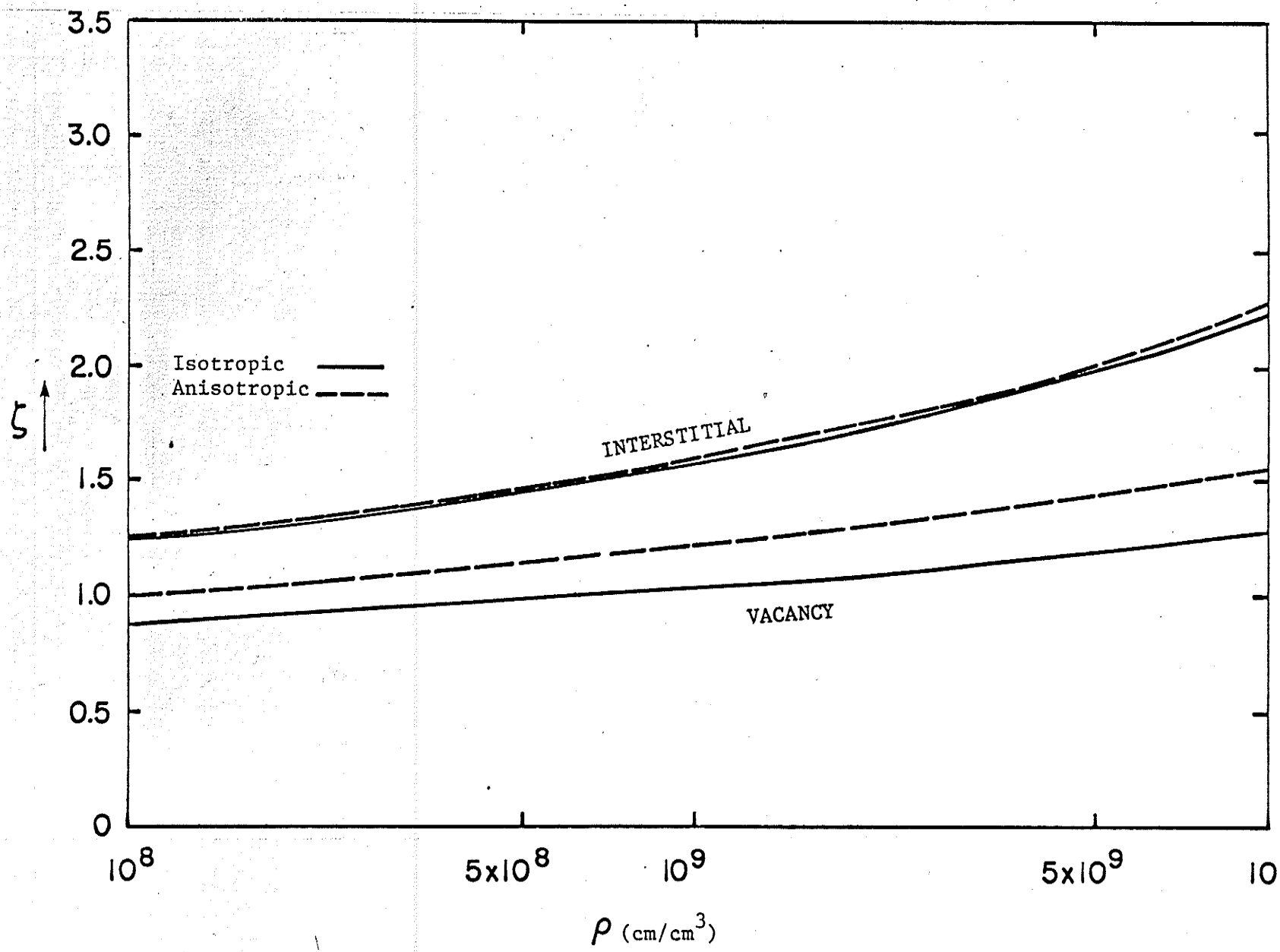

FIGURE 1: Edge Dislocation Sink Strengths for Isotropic and Anisotropic Point Defects in Copper at 500 K. Dipole tensors for the anisotropic point defects are calculated using the MM interatomic potential.

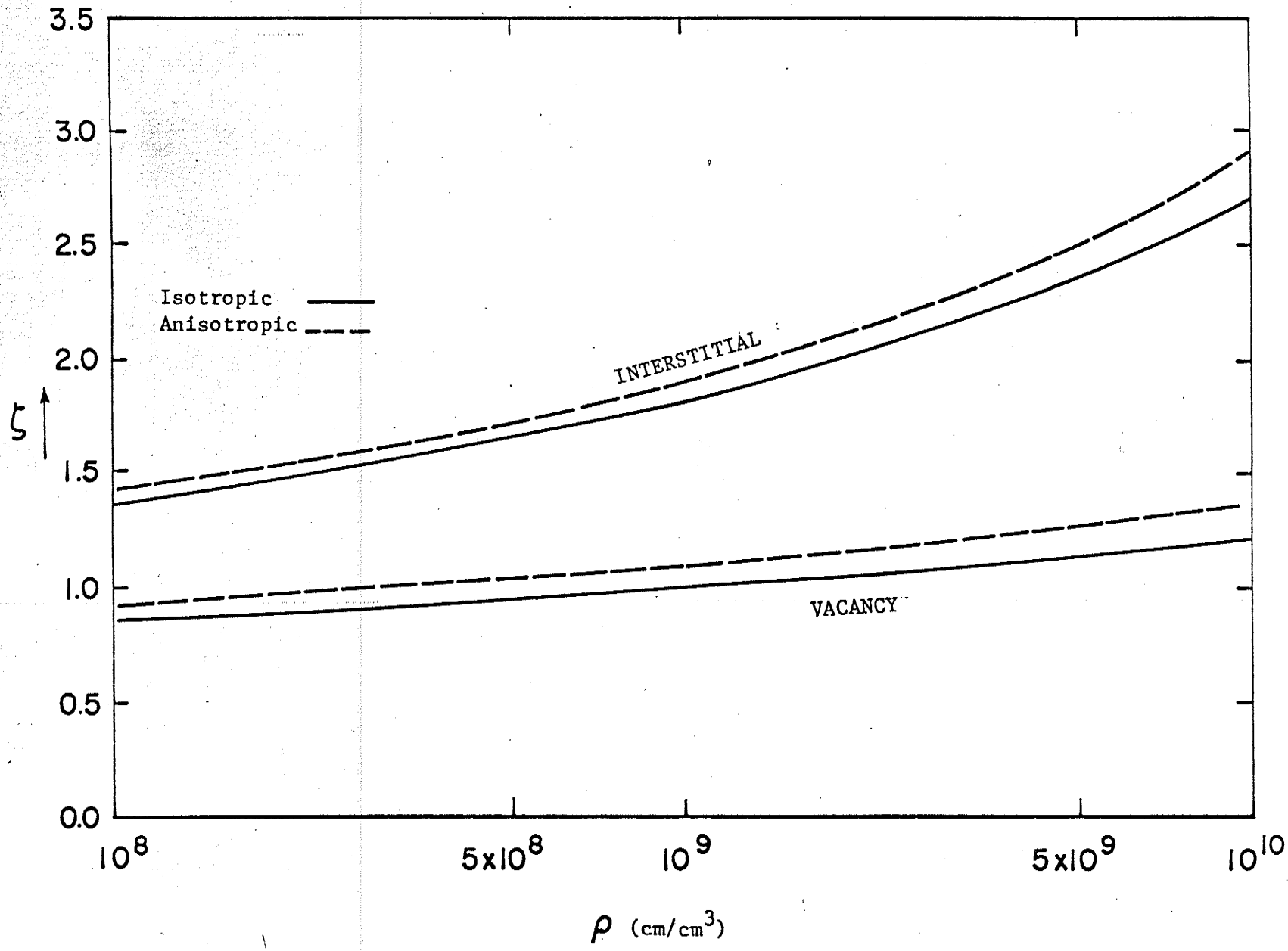

FIGURE 2: Edge Dislocation Sink Strengths for Isotropic and Anisotropic Point Defects in Iron at 500 K. Dipole tensors for the anisotropic point defects are calculated using the Johnson interatomic potential.

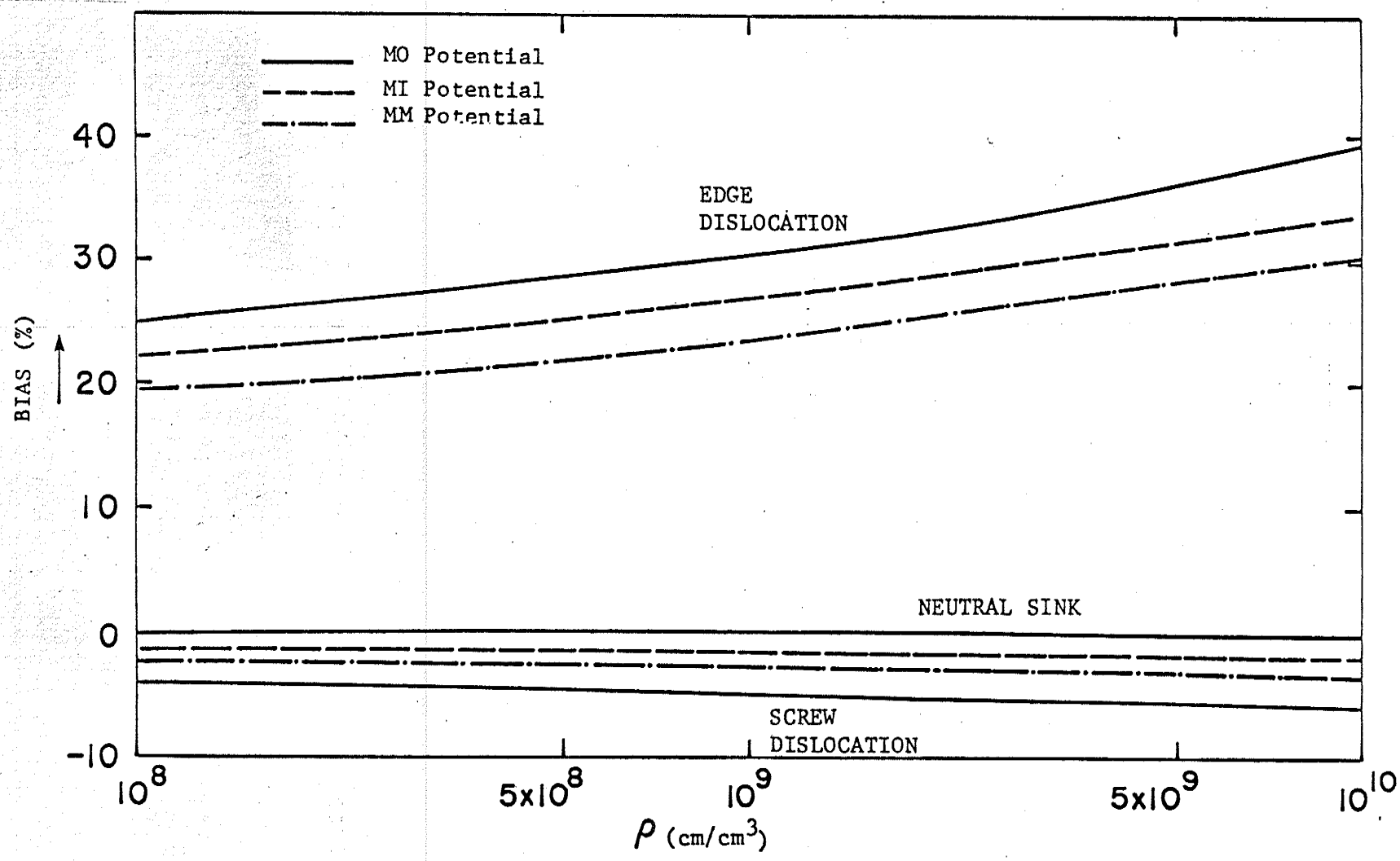

FIGURE 3: Stress-Free Biases of Dislocations in Copper at 500 K for Three Modified Morse Interatomic Potentials

because of this point-defect segregation. Bias versus dislocation line density, for both types of dislocations in iron, has been plotted in Figure 4. As in copper, the edge dislocation has a strong bias for interstitials. However, the screw dislocation may be a significant sink in iron. It is also strongly biased toward interstitials, and thus can be an important factor in irradiation damage studies in iron.

The effect of the external applied stress can be seen from the values of the stress coefficients, ΔT_α. To get some idea of the significance of this effect, it is instructive to compare these results with the corresponding quantity ΔW_α, due to SIPA-I. Of course, such a comparison is valid only for edge dislocations, because the screw dislocation is usually assumed to be an unbiased sink. If we assume that the interstitial at the saddle point is soft in shear, then the change in sink strength due to SIPA-I is given by equations (74) to (76). For the purpose of the present comparison, we assume that $\zeta(0)/\epsilon_i \simeq 1$.

The SIPA-SAPSE coefficients are compared with the SIPA-I coefficients for copper and iron in Table 3 and Table 4, respectively, for a temperature of 500 K and a dislocation line density of 10^{10} cm/cm^3. These coefficients are essentially independent of the dislocation line density. For copper, two features are immediately apparent. First, comparing the ΔT's and the ΔW's, it can be seen that the effect of an externally applied stress on the bias of an edge dislocation due to SIPA-SAPSE is opposite in sign to that due to SIPA-I. Second, for SIPA-I, the dominant orientation factor is ΔW_β which relates to the orientation of the stress with respect to the Burgers vector. For SIPA-SAPSE, this coefficient is essentially negligible compared with the coefficient ΔT_λ for the orientation of the

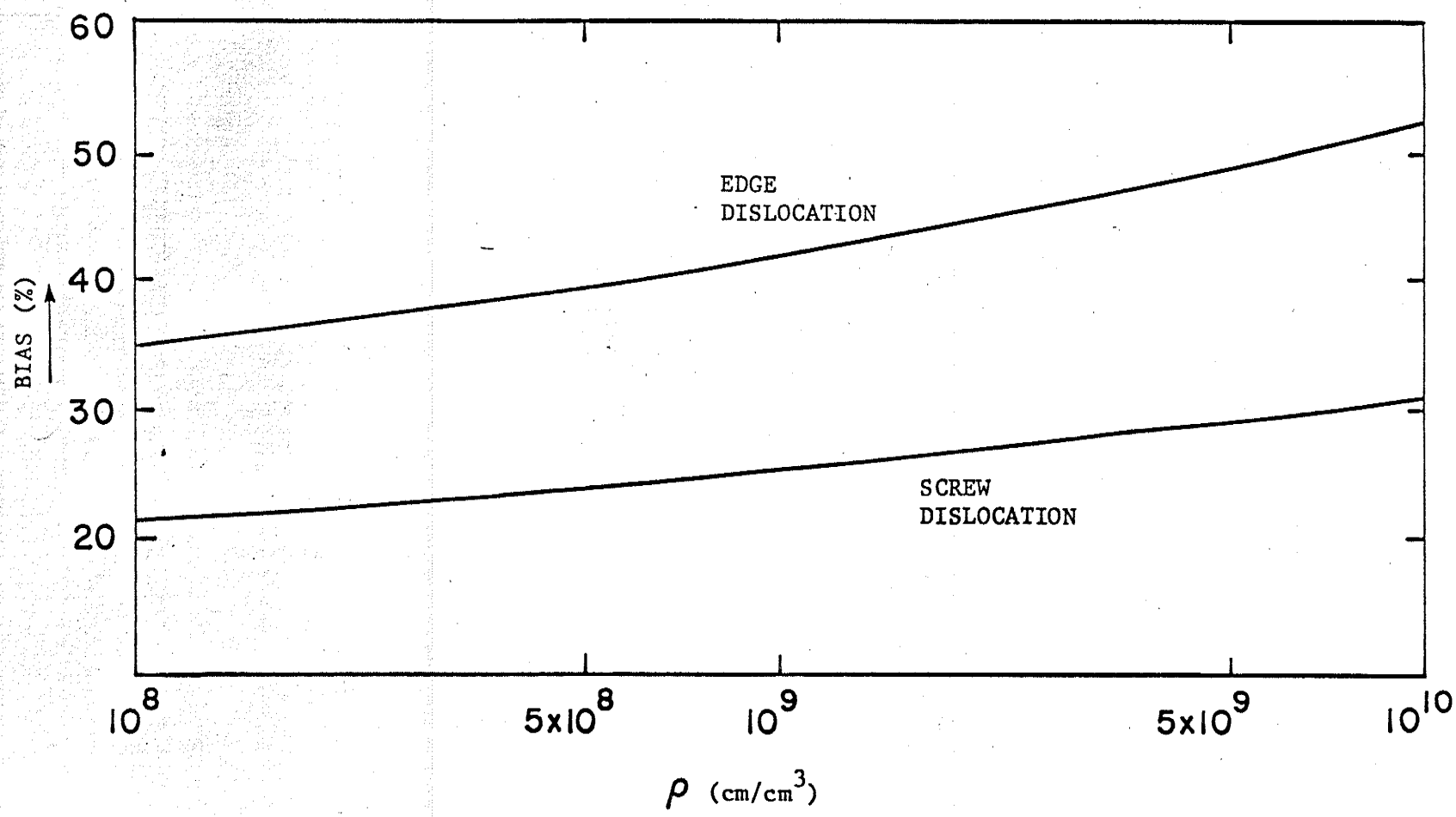

FIGURE 4: Stress-Free Biases of Dislocations in Iron at 500 K for the Johnson Interatomic Potential

TABLE 3

STRESS DEPENDENCE COEFFICIENTS* FOR STRAIGHT DISLOCATIONS IN COPPER AT 500 K AND $\rho = 10^{10}$ cm/cm^3

	SIPA-SAPSE							SIPA-I			
		VACANCY		INTERSTITIAL				$\Delta\mu_i = -1$		$\Delta\mu_i = -0.5$	
POTENTIAL	ΔT_λ^S	H_β^E	H_λ^E	H_β^E	H_λ^E	ΔT_β^E	ΔT_λ^E	ΔW_β	ΔW_λ	ΔW_β	ΔW_λ
M0	-6.95	6.54	29.51	247.32	577.54	-0.49	-6.90	0.47	0.16	0.17	0.06
M1	-5.65	1.25	15.07	77.91	248.60	-0.22	-5.57	0.47	0.16	0.17	0.06
MM	-7.17	3.12	25.88	53.72	243.01	-0.23	-7.00	0.47	0.16	0.17	0.06

TABLE 4

STRESS DEPENDENCE COEFFICIENTS* FOR STRAIGHT DISLOCATIONS IN IRON AT 500 K AND $\rho = 10^{10}$ cm/cm^3

	SIPA-SAPSE							SIPA-I			
		VACANCY		INTERSTITIAL				$\Delta\mu_i = -1$		$\Delta\mu_i = -0.5$	
POTENTIAL	ΔT_λ^S	H_β^E	H_λ^E	H_β^E	H_λ^E	ΔT_β^E	ΔT_λ^E	ΔW_β	ΔW_λ	ΔW_β	ΔW_λ
JOHNSON	-15.91	-7.43	4.51	-355.33	771.83	1.64	-14.28	0.45	0.13	0.15	0.05

*see Equations 70-76 for definition

stress with respect to the line direction. Further, the magnitude of ΔT_λ is an order of magnitude greater than that of ΔW_β for SIPA-I. For iron, we see that both ΔT_β and ΔW_β have the same sign. But, for SIPA-SAPSE, ΔT_λ is the dominant orientation factor and has the opposite sign to ΔW_λ for SIPA-I. ΔT_λ for SIPA-SAPSE could be up to two orders of magnitude greater than ΔW_β for SIPA-I.

Figure 5 illustrates the orientation dependence more clearly. It emphasizes the fact that the dominant factor is the orientation of the stress with respect to the line direction. This is in qualitative agreement with the numerical solution of Tomé et al. [18], who also found a large line direction dependence. Quantitative agreement is difficult to obtain at the high dislocation line density and high applied stress level for which they report results, because of differences in the model for calculating the currents and because of the non-linear stress dependence at high applied stress levels.

In the last section, we mentioned that one may approximate an edge dislocation loop by averaging the line direction of an edge dislocation in a plane to which the Burgers vector is normal. Using this approximation, ΔT_β for the finite loop can be calculated. The results are presented in Table 5. The results from the SIPA-I theory are included as well as results for the infinitesimal edge dislocation loop [16], for comparison. It can be seen that values of ΔT_β due to SAPSE for the infinitesimal and finite loop cases, are quite similar, with the infinitesimal loop results about 30% higher in all cases. Comparison with the SIPA-I results, however, shows that the magnitude of the SIPA-SAPSE effect is 5 to 25 times larger than that of SIPA-I. In this connection, the SIPA effect in loops, as observed experimentally by Garner, Wolfer and Brager [26], may be a con-

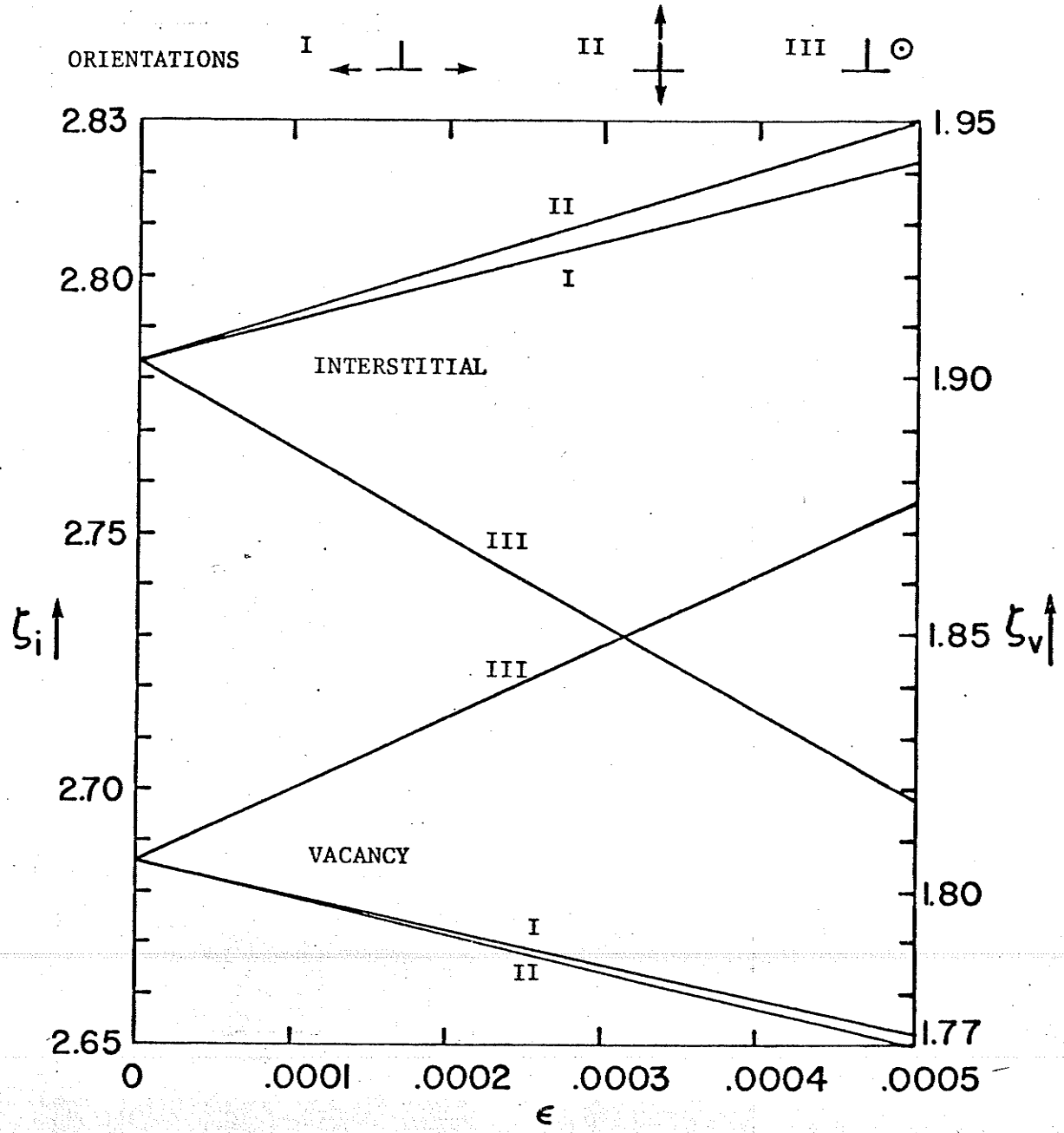

FIGURE 5: Edge Dislocation Sink Strengths as a Function of Externally Applied Uniaxial Strain, ϵ, at 300 K and a Dislocation Line Density of 10^{10} cm/cm^3. Three orientations of the uniaxial strain axis are considered: Orientation I is parallel to the Burgers vector of the edge dislocation, Orientation II is perpendicular to the Burgers vector and the line direction, and Orientation III is parallel to the line direction.

TABLE 5

COMPARISON OF SIPA-SAPSE AND SIPA-I STRESS COEFFICIENTS FOR DISLOCATION LOOPS IN COPPER AND IRON AT 500 K AND $\rho = 10^{10}$ cm/cm^3

		SIPA-SAPSE			SIPA-I	
		Finite Loop	IEDL			
Material	Potential	ΔT_β	ΔT_β^{vL}	ΔT_β^{iL}	ΔW_β ($\Delta\mu_i$=-1)	ΔW_β ($\Delta\mu_i$=-0.5)
Copper	M0	2.97	4.12	3.16	0.39	0.14
Copper	M1	2.57	3.78	3.18	0.39	0.14
Copper	MM	3.27	-	-	0.39	0.14
Iron	Johnson	8.78	11.72	17.10	0.39	0.14

sequence of SAPSE rather than due to the elastic polarizability of the point defect. Since the SIPA-SAPSE effect in loops is mainly a consequence of the line direction dependence of the dislocation sink strength, it follows that SIPA-SAPSE in loops depends more on the relative orientation with respect to the stress direction of the loop-plane normal rather than the Burgers vector, which happens to be in the same direction as the loop-plane normal in the case of an edge dislocation loop. This may be an important point that may permit experimental discrimination between the two SIPA effects.

Chapter 6

SUMMARY AND CONCLUSIONS

The effects of the anisotropy of the saddle-point configurations of point defects (SAPSE) have been studied in this report. Expressions for both the sink strengths and the biases of infinite straight edge and screw dislocations in an isotropic linear elastic medium have been calculated. From these expressions, we can come to several general conclusions. First, SAPSE does not significantly affect the magnitude of the dislocation sink strengths. However, a screw dislocation will be a biased sink for anisotropic vacancies and interstitials. In copper this bias is very small, but in iron it is quite large and, hence, may have to be considered in irradiation damage studies. Second, the application of an external stress changes the bias in a way similar to the usual SIPA for edge dislocations (SIPA-I), in that the change is proportional to $\frac{\sigma}{\mu}$ and they both have a similar dependence on the orientation of the applied stress, with respect to the Burgers vector direction and the line direction. SIPA-SAPSE applies to both screw and edge dislocations. However, unlike SIPA-I, in SIPA-SAPSE the important factor is the orientation of the stress with respect to the line direction, rather than the Burgers vector direction. The sign of the change in the sink strength is a function of the saddle-point shape of the point defect, i.e., whether it is elongated or flattened in the jump direction. The magnitude of the change in SIPA-SAPSE is more than an order of magnitude larger than that in SIPA-I for copper and iron. Furthermore, the change in the sink strength depends on temperature and point-defect size differently in the two SIPA mechanisms. In the SAPSE case, the change varies inversely with temperature explicitly and varies directly with the point-defect size, while in the SIPA-I case, the change with temperature varies as the dislo-

cation sink strength temperature dependence and varies inversely with the point-defect size.

The SAPSE on the point-defect drift-diffusion to a finite dislocation loop has also been studied approximately by averaging over the line direction. For iron and copper, SIPA-SAPSE is also much larger than that of SIPA-I. It is postulated that if SIPA-SAPSE is the governing SIPA mechanism, the SIPA effect would depend mainly on the relative orientation with respect to the applied stress direction of the loop-plane normal rather than the Burgers vector.

REFERENCES

1. H. Ullmaier and W. Schilling, "Radiation Damage in Metallic Reactor Materials", in Physics of Modern Materials, p. 301, International Atomic Energy Agency, Vienna, 1980.

2. P.T. Heald and M.V. Speight, "Steady-State Irradiation Creep", Phil. Mag. 29, 1075 (1974).

3. R. Bullough and J.R. Willis, "The Stress-Induced Point Defect - Dislocation Interaction and its Relevance to Irradiation Creep", Phil. Mag. 31, 855 (1975).

4. C.H. Woo, "Effects of an Anisotropic Dislocation Structure on Irradiation Creep Due to Stress-Induced Preferred Absorption of Point Defects", J. Nucl. Mater. 80, 132 (1979).

5. C.H. Woo, "Irradiation Creep Due to Climb-Induced Glide in an Anisotropic Dislocation Structure", J. Nucl. Mater. 98, 295 (1981).

6. W.G. Wolfer and M. Ashkin, "Diffusion of Vacancies and Interstitials to Edge Dislocations", J. Appl. Phys. 47, 791 (1976).

7. L.A. Girifalco and D.O. Welch, Point Defects and Diffusion in Strained Metals, Gordon and Breach, New York, 1967.

8. H. Kronmuller, W. Frank, and W. Hornung, "Diffusion of Anisotropic Point Defects in Cubic Crystals in the Presence of a Field of Force", Phys. Stat. Sol. (b) 46, 165 (1971).

9. E.J. Savino, "Point Defect - Dislocation Interaction in a Crystal Under Tension", Phil. Mag. 36, 323 (1977).

10. P.H. Dederichs and K. Schroeder, "Anisotropic Diffusion in Stress Fields", Phys. Rev. B 17, 2524 (1978).

11. W.G. Wolfer and M. Ashkin, "Stress-Induced Diffusion of Point Defects to Spherical Sinks", J. Appl. Phys. 46, 547 (1975).

12. K. Schroeder and K. Dettmann, "Diffusion Reactions in Long Range Potentials", Z. Phys. B 22, 343 (1975).

13. H.R. Schober, "Single and Multiple Interstitials in FCC Metals", J. Phys. F 7, 1127 (1977).

14. P.H. Dederichs, C. Lehmann, H.R. Schober, A. Scholz, and R. Zeller, "Lattice Theory of Point Defects", J. Nucl. Mat. 69 & 70, 176 (1978).

15. C.K. Ong, J.M. Vail and C.H. Woo, "Computer Simulation of Point Defects in Metals", unpublished Whiteshell Nuclear Research Establishment Report, WNRE-198 (1982).

16. C.H. Woo, (a) "Point Defect Migration Into an Infinitesimal Dislocation Loop: Effects of the Anisotropy of the Saddle-Point Configuration", Atomic Energy of Canada Limited Report, AECL-6819 (1981); (b) J. Nucl. Mater. 107, 20 (1982).

17. R. Bullough and R.C. Newman, "The Kinetics of Migration of Point Defects to Dislocations", Rep. Prog. Phys., 33, 101 (1970).

18. C.N. Tomé, H.A. Ceccatto, and E.J. Savino, "Point Defect Diffusion in a Strained Crystal", Phys. Rev. 25 (1982) 7428.

19. R. Bullough, D.W. Wells, J.R. Willis, and M.H. Wood, "The Interaction Energy Between Interstitial Atoms and Dislocations and its Relevance to Irradiation Damage", in Proceedings of the International Conference on Dislocation Modelling of Physical Systems (Gainesville, Florida (1980)), Pergamon Press, Oxford, 1981.

20. W.A. Coghlon, "Transient and Steady State Diffusion Solution for Point Defects in a Stress Field", in Proceedings of Conference on Computer Simulation for Materials Applications, (National Bureau of Standards, Gaithersburg, MD (1976)) Nuclear Metallurgy 20, part 1, 166.

21. M.H. Yoo and W.H. Butler, "Steady-State Diffusion of Point Defects in the Interaction Force Field", Phys. Stat. Sol. 77, 181 (1976).

22. C.H. Woo, "The Sink Strength of a Dislocation Loop in the Effective Medium Approximation", J. Nucl. Mater. 98, 279 (1981).

23. P.T. Heald and M.V. Speight, "Point Defect Behaviour in Irradiated Materials", Acta Met. 23, 1389 (1975).

24. J.P. Hirth and J. Lothe, Theory of Dislocations, McGraw-Hill, New York, 1968.

25. C.H. Woo, a) "Irradiation Deformation Due to SIPA Induced Dislocation Anisotropy", Atomic Energy of Canada Limited Report, AECL-6791, (1980), b) Phil. Mag. 42, 551 (1980).

26. F.A. Garner, W.G. Wolfer and H.R. Brager, Journal of Testing and Evaluation, ASTM, STP 683, 160 (1979).

APPENDIX A

DERIVATION OF EXPRESSION FOR SINK STRENGTH OF A CYLINDRICAL SINK USING THE CONSTANT BOUNDARY CONCENTRATION METHOD

Here we wish to solve the differential equation

$$\underset{\sim}{\nabla} \cdot D_o^{eff} g(r) \cdot \underset{\sim}{\nabla} n(r) = 0 \tag{A-1}$$

subject to the boundary conditions

$$n(r_o) = C^e \tag{A-2}$$

and

$$n(R) = \bar{C}. \tag{A-3}$$

Note that equation (A-3) is derived from an assumption that R is sufficiently large so that $E_g(R) \to 0$. The solution of equation (A-1), subject to boundary conditions given by equations (A-2) and (A-3), is

$$n(r) = \alpha(\bar{C}-C^e) \int^r \frac{dt}{tg(t)} \tag{A-4}$$

where

$$\alpha = \left[\int_{r_o}^{R} \frac{dt}{tg(t)} \right]^{-1} . \tag{A-5}$$

The current density is given by

$$\underset{\sim}{j} = \frac{1}{\Omega} g(r) \underset{\sim}{\nabla} [D_o^{eff} n(r)] \tag{A-6}$$

$$= \frac{D_o^{eff}}{\Omega} (\bar{C}-C^e) \frac{\alpha \underset{\sim}{\hat{r}}}{r} .$$

The current into a cylinder of radius r and unit length is

$$i = \int \underset{\sim}{j} \cdot d\underset{\sim}{s} = \frac{D_o^{eff}(\bar{C}-C^e)}{\Omega} 2\pi\alpha . \tag{A-7}$$

The current through a unit volume is given by

$$I = i\rho . \tag{A-8}$$

where ρ is the dislocation density. The current through a unit volume can also be written as

$$I = D_o^{eff} \frac{(\bar{C}-C^e)}{\Omega} k^2 \qquad \text{(A-9)}$$

where k^2 is called the sink strength. A comparison of equations (A-8) and (A-9), using equations (A-5) and (A-7), reveals that

$$\frac{k^2}{\rho} = 2\pi \Big/ \int_{r_o}^{R} \frac{dt}{tg(t)} \quad . \qquad \text{(A-10)}$$

APPENDIX B

RELATIONSHIP OF $\underset{\sim}{e}^{(2)}$ AND $\underset{\sim}{e}^{(3)}$ IN TERMS OF $\underset{\sim}{e}^{(1)}$

Let θ, ϕ, and ψ be the three Eulerian angles [B.1] between the basis sets $\underset{\sim}{e}^{(n)}$ and the x-y-z cartesian coordinate system. In terms of cartesian coordinates, $\underset{\sim}{e}^{(n)}$ can be expressed as the following column vectors

$$\underset{\sim}{e}^{(1)} = \begin{pmatrix} \sin\theta\cos\phi \\ \sin\theta\sin\phi \\ \cos\theta \end{pmatrix}, \quad \underset{\sim}{e}^{(2)} = \begin{pmatrix} \sin\phi\cos\psi + \cos\theta\cos\phi\sin\psi \\ -\cos\phi\cos\psi + \cos\theta\sin\phi\sin\psi \\ -\sin\theta\sin\psi \end{pmatrix},$$

$$\underset{\sim}{e}^{(3)} = \begin{pmatrix} -\sin\phi\sin\psi + \cos\theta\cos\phi\cos\psi \\ \cos\phi\sin\psi + \cos\theta\sin\phi\cos\psi \\ -\sin\theta\cos\psi \end{pmatrix}.$$

We can now evaluate $e_i^{(2)}e_j^{(2)}$ from the elements of $\underset{\sim}{e}^{(2)}$. In the above description, the angle ψ represents a rotation about $\underset{\sim}{e}^{(1)}$. For simplicity, we assume that ψ is distributed randomly, so that we may average over ψ and assume $\cos^2\psi = \sin^2\psi = \frac{1}{2}$ and $\cos\psi\sin\psi = 0$. Then $e_i^{(2)}e_j^{(2)}$ becomes

$$e_i^{(2)}e_j^{(2)} = \frac{1}{2}\begin{pmatrix} \sin^2\phi+\cos^2\theta\cos^2\phi & \cos\phi\sin\phi(\cos^2\theta-1) & -\cos\theta\sin\theta\cos\phi \\ & \cos^2\phi+\cos^2\theta\sin^2\phi & -\cos\theta\sin\theta\sin\phi \\ \text{symmetrical} & & \sin^2\theta \end{pmatrix}$$

$$= \frac{1}{2}(\delta_{ij} - e_i^{(1)}e_j^{(1)}). \qquad \text{(B-1)}$$

Similarly, we can show

$$e_i^{(3)}e_j^{(3)} = \frac{1}{2}(\delta_{ij} - e_i^{(1)}e_j^{(1)}). \qquad \text{(B-2)}$$

Using equations (B.1) and (B.2), we can combine the expressions for $e_i^{(1)}e_j^{(1)}$, $e_i^{(2)}e_j^{(2)}$, and $e_i^{(3)}e_j^{(3)}$ into the following general expression in terms of $e_i^{(1)}e_j^{(1)}$

$$e_i^{(n)}e_j^{(n)} = \delta_{n1}e_i^{(1)}e_j^{(1)} + \frac{1}{2}(\delta_{n2} + \delta_{n3})(\delta_{ij} - e_i^{(1)}e_j^{(1)})$$

(no implied summation)

$$= \frac{1}{2}[e_i^{(1)}e_j^{(1)}(3\delta_{n1}-1) + \delta_{ij}(1-\delta_{n1})] \; . \qquad \text{(B.3)}$$

REFERENCES

B.1 H. Goldstein, Classical Mechanics, 2nd Edition, Addison-Wesley, Cambridge, Mass., 1980.

APPENDIX C

EVALUATION OF g(r) FOR AN EDGE DISLOCATION

g(r) for an edge dislocation is given by

$$g(r) = \frac{3}{2\pi}\int_0^{2\pi} \hat{r}_\mu \hat{r}_\nu \exp(\beta P e_{kk})\gamma(\mu,\nu)d\theta_r$$

$$+ \frac{3}{2\pi}\sum_{m=1}^{\infty}\frac{1}{m!}\left[\frac{3}{2}\beta P(p_1-1)\right]^m \int_0^{2\pi} \hat{r}_\mu \hat{r}_\nu \exp(\beta P e_{kk}) \qquad \text{(C-1)}$$

$$\cdot f_{i_1 j_1} f_{i_2 j_2} \cdots f_{i_m j_m} \gamma(\mu,\nu,i_1,j_1,\ldots i_m,j_m)d\theta_r \ .$$

The γ values can be determined using the solution in Appendix B of reference 16(a) with the result that

$$g(r) = T_1 + T_2 + T_3 + O(r^{-4}) \qquad \text{(C-2)}$$

where

$$T_1 = \frac{1}{2\pi}\int_0^{2\pi} \exp(F\frac{b}{r}\hat{y})d\theta_r \ , \qquad \text{(C-3a)}$$

$$T_2 = \frac{1}{20\pi}(p_1-1)F\frac{b}{r}\int_0^{2\pi} \hat{y}\exp(F\frac{b}{r}\hat{y})d\theta_r \ , \qquad \text{(C-3b)}$$

$$T_3 = \frac{1}{560\pi}(p_1-1)^2\left[F\frac{b}{r}\right]^2 \int_0^{2\pi} \left[5\hat{y}^2 + \frac{27}{(1-2\nu)^2}\hat{x}^2\right]\exp(F\frac{b}{r}\hat{y})d\theta_r \ , \qquad \text{(C-3c)}$$

and

$$F = -\frac{(1-2\nu)\beta P}{2\pi(1-\nu)} \ . \qquad \text{(C-4)}$$

These integrals can be evaluated with the aid of tables of integrals [C.1]:

$$T_1 = 1 + \sum_{m=1}^{\infty}\frac{1}{[(2m)!!]^2}\left(F\frac{b}{r}\right)^{2m} \ , \qquad \text{(C-5a)}$$

$$T_2 = \frac{1}{5}(p_1-1) \sum_{m=1}^{\infty} \frac{m}{[(2m)!!]^2} [F\frac{b}{r}]^{2m} \quad , \tag{C-5b}$$

$$T_3 = \frac{1}{140}(p_1-1)^2 \sum_{m=1}^{\infty} \frac{m}{[(2m)!!]^2} [F\frac{b}{r}]^{2m} [5(2m-1) + \frac{27}{(1-2\nu)^2}] \quad , \tag{C-5c}$$

and

$$(2m)!! = 2m\cdot(2m-2)\ldots 2 \quad . \tag{C-6}$$

Substituting equations (C-5a) to (C-5c) into equation (C-2) we obtain

$$g(r) = 1 + F^E(\frac{b}{r})^2 + O(r^{-4}) \tag{C-7}$$

where

$$F^E = \frac{\beta^2 P^2 (1-2\nu)^2}{16\pi^2(1-\nu)^2} [1 + \frac{1}{5}(p_1-1) + \frac{1}{140}\{5 + \frac{27}{(1-2\nu)^2}\}(p_1-1)^2] \quad . \tag{C-8}$$

REFERENCES

C.1 I.F. Gradshteyn and I.M. Ryzhik, "Table of Integrals, Series and Products", Academic Press, New York (1965), 4th Edition.

APPENDIX D

EVALUATION OF g(r) FOR A SCREW DISLOCATION

g(r) for a screw dislocation is given by

$$g(r) = \frac{3}{2\pi}\int_0^{2\pi} d\theta_r \int \frac{d\Omega_h}{4\pi}(\hat{r}\cdot\hat{h})^2 \exp\left(\frac{1}{2}A\frac{b}{r}G_{\mu\nu}\hat{r}_\mu\hat{h}_\nu\hat{h}_3\right) \quad , \tag{D-1}$$

where

$$A = \frac{3\beta P}{2\pi}(p_1-1) \quad . \tag{D-2}$$

Expanding the exponential in an infinite series, we obtain

$$g(r) = \frac{3}{2\pi}\int_0^{2\pi} \hat{r}_\mu\hat{r}_\nu\gamma(\mu,\nu)d\theta_r$$

$$+ \frac{3}{2\pi}\sum_{m=1}^{\infty}\frac{1}{m!}\left(\frac{1}{2}A\frac{b}{r}\right)^m \int_0^{2\pi} G_{\mu_1\nu_1}G_{\mu_2\nu_2}\cdots G_{\mu_m\nu_m} \tag{D-3}$$

$$\cdot \hat{r}_\mu\hat{r}_\nu\hat{r}_{\mu_1}\hat{r}_{\mu_2}\cdots\hat{r}_{\mu_m}\gamma(\mu,\nu,\nu_1,\nu_2,\ldots,\nu_m,\overbrace{3,3,\ldots,3}^{m})d\theta_r$$

The γ values can be determined using the solution in Appendix B of reference 16(a) and using the identities given by equation (37) we obtain

$$g(r) = 6\sum_{m=0}^{\infty}\frac{[(2m+1)!!]^2}{(2m+1)(4m+3)!}A^{2m}\left(\frac{b}{r}\right)^{2m} \tag{D-4}$$

where

$$(2m+1)!! = (2m+1)\cdot(2m-1)\ldots 1 \quad . \tag{D-5}$$

APPENDIX E

EVALUATION OF g'(r) FOR AN EDGE DISLOCATION

g'(r) for an edge dislocation is given by

$$g'(r) = \frac{9}{2}\beta P(p_1-1)\int\frac{d\Omega_h}{4\pi}\int_0^{2\pi}\frac{d\theta_r}{2\pi}(\hat{r}\cdot\hat{h})^2(s_n t_i^{(n)} t_j^{(n)}\hat{h}_i\hat{h}_j - 1)\exp[-\beta E_s^i(\underset{\sim}{r},\hat{h})], \quad \text{(E-1)}$$

$$= \frac{9}{2}\beta P(p_1-1)\{\int\frac{d\Omega_h}{4\pi}\int_0^{2\pi}\frac{d\theta_r}{2\pi}(\hat{r}\cdot\hat{h})^2 s_n t_i^{(n)} t_j^{(n)}\hat{h}_i\hat{h}_j\exp[-\beta E_s^i(\underset{\sim}{r},\hat{h})] \quad \text{(E-2)}$$

$$- \frac{1}{3}g(r)\Big|_{\varepsilon=0}\} .$$

Substituting for $E_s^i(\underset{\sim}{r},\hat{h})$ (see equations (25) and (28)) we obtain

$$g'(r) = \frac{9}{2}\beta P(p_1-1)\{\frac{1}{2\pi}s_n\hat{t}_i^{(n)}\hat{t}_j^{(n)}\int_0^{2\pi}\hat{r}_\mu\hat{r}_\nu\exp(\beta P e_{kk})\gamma(\mu,\nu,i,j)d\theta_r$$

$$+ \frac{1}{2\pi}s_n\hat{t}_i^{(n)}t_j^{(n)}\sum_{m=1}^{\infty}\frac{1}{m!}[\frac{3}{2}\beta P(p_1-1)]^m\int_0^{2\pi}\hat{r}_\mu\hat{r}_\nu\exp(\beta P e_{kk}) \quad \text{(E-3)}$$

$$\cdot f_{i_1 j_1}f_{i_2 j_2}\cdots f_{i_m}f_{j_m}\gamma(\mu,\nu,i,j,i_1,j_1,\ldots,i_m,j_m)d\theta_r$$

$$- \frac{1}{3}g(r)\Big|_{\varepsilon=0}\} .$$

The γ values can be determined using the solution in Appendix B of reference 16(a) with the result that

$$g'(r) = \frac{9}{2}\beta P(p_1-1)[T_1^\varepsilon + T_2^\varepsilon + T_3^\varepsilon - \frac{1}{3}g(r)\Big|_{\varepsilon=0}] + O(r^{-4}) \quad \text{(E-4)}$$

where

$$T_1^\varepsilon = \frac{1}{5}T_1 + \frac{2}{15}s_n[t_1^{(n)}]^2 I_{02} + \frac{2}{15}s_n[t_2^{(n)}]^2 I_{20} , \quad \text{(E-5a)}$$

$$T_2^{\varepsilon} = \frac{2}{7}T_2 + \frac{1}{105}\frac{(11-4\nu)}{(1-2\nu)}(p_1-1)F\frac{b}{r}s_n[t_1^{(n)}]^2 I_{12}$$

$$+ \frac{1}{105}\frac{1}{(1-2\nu)}(p_1-1)F\frac{b}{r}s_n[t_2^{(n)}]^2\{2(1-2\nu)I_{30}-9I_{12}\} - \frac{1}{70}(p_1-1)F\frac{b}{r}s_n[t_3^{(n)}]^2 I_{10} \quad , \tag{E-5b}$$

$$T_3^{\varepsilon} = \frac{1}{9}T_3 + \frac{1}{3780(1-2\nu)^2}(p_1-1)^2(F\frac{b}{r})^2\{s_n[t_1^{(n)}]^2[45I_{04}+(18+54(1-2\nu)+9(1-2\nu)^2)I_{22}$$

$$+ 9I_{02}+2(1-2\nu)^2 I_{20}]+s_n[t_2^{(n)}]^2[18I_{04}+(45-54(1-2\nu))I_{22}+9(1-2\nu)^2 I_{40} \tag{E-5c}$$

$$+ 9I_{02}+2(1-2\nu^2)I_{20}]+s_n[t_3^{(n)}]^2 2(1-2\nu)^2 I_{20} \quad .$$

where T_1, T_2 and T_3 are given by equations (C-3a) to (C-3c) in Appendix C. F is given by equation (C-4) in Appendix C, and

$$I_{ab} = \frac{1}{2\pi}\int_0^{2\pi} \hat{y}^a\hat{x}^b \exp(F\frac{b}{r}\hat{y})\, d\theta_r \quad . \tag{E-6}$$

These integrals can be evaluated with the aid of tables of integrals [E.1]:

$$I_{10} = \frac{1}{2}F\frac{b}{r}\sum_{m=0}^{\infty}\frac{1}{[(2m)!!]^2}(F\frac{b}{r})^{2m}\frac{1}{(m+1)} \quad , \tag{E-7a}$$

$$I_{20} = \frac{1}{2}\sum_{m=0}^{\infty}\frac{1}{[(2m)!!]^2}(F\frac{b}{r})^{2m}\frac{(2m+1)}{(m+1)} \quad , \tag{E-7b}$$

$$I_{30} = \frac{1}{4}F\frac{b}{r}\sum_{m=0}^{\infty}\frac{1}{[(2m)!!]^2}(F\frac{b}{r})^{2m}\frac{(2m+3)}{(m+2)(m+1)} \quad , \tag{E-7c}$$

$$I_{40} = \frac{1}{4}\sum_{m=0}^{\infty}\frac{1}{[(2m)!!]^2}(F\frac{b}{r})^{2m}\frac{(2m+3)(2m+1)}{(m+2)(m+1)} \quad , \tag{E-7d}$$

$$I_{02} = \frac{1}{2}\sum_{m=0}^{\infty}\frac{1}{[(2m)!!]^2}(F\frac{b}{r})^{2m}\frac{1}{(m+1)} \quad , \tag{E-7e}$$

$$I_{12} = \frac{1}{4}F\frac{b}{r}\sum_{m=0}^{\infty}\frac{1}{[(2m)!!]^2}(F\frac{b}{r})^{2m}\frac{1}{(m+2)(m+1)} \quad , \tag{E-7f}$$

$$I_{22} = \frac{1}{4} \sum_{m=0}^{\infty} \frac{1}{[(2m)!!]^2} \left(F\frac{b}{r}\right)^{2m} \frac{(2m+1)}{(m+2)(m+1)} \quad , \tag{E-7g}$$

$$I_{04} = \frac{3}{4} \sum_{m=0}^{\infty} \frac{1}{[(2m)!!]^2} \left(F\frac{b}{r}\right)^{2m} \frac{1}{(m+2)(m+1)} \quad , \tag{E-7h}$$

and

$$(2m)!! = (2m)\cdot(2m-2)\ldots 2 \quad . \tag{E-8}$$

We also note the following identities:

$$t_1^{(n)} = \cos \beta_n \quad , \tag{E-9a}$$

$$t_3^{(n)} = \cos \lambda_n \quad , \tag{E-9b}$$

$$t_2^{(n)} = \sqrt{1 - \cos^2\beta_n - \cos^2\lambda_n} \quad , \tag{E-9c}$$

where β_n is the angle between the Burgers vector of the edge dislocation and the nth principal direction of the externally applied stress, and λ_n is the angle between the line direction of the edge dislocation and the nth principal direction of the externally applied stress.

Substituting equations (E-7) and (E-9) into equations (E-5), we obtain

$$T_1^{\varepsilon} = \frac{1}{3}T_1 + \frac{1}{15}(1-s_n\cos^2\lambda_n) + \frac{1}{30}\left(F\frac{b}{r}\right)^2(1-s_n\cos^2\beta_n)$$

$$\cdot \sum_{m=0}^{\infty} \frac{1}{[(2m)!!]^2} \frac{1}{(m+2)(m+1)} \left(F\frac{b}{r}\right)^{2m} \tag{E-10a}$$

$$+ \frac{1}{60}\left(F\frac{b}{r}\right)^2(1-s_n\cos^2\lambda_n) \sum_{m=0}^{\infty} \frac{1}{[(2m)!!]^2} \frac{(2m+3)}{(m+2)(m+1)^2} \left(F\frac{b}{r}\right)^2 \quad ,$$

$$T_2^{\varepsilon} = \frac{1}{3}T_2 + \frac{1}{210}(p_1-1)\left(F\frac{b}{r}\right)^2(1-s_n\cos^2\beta_n) \sum_{m=0}^{\infty} \frac{1}{[(2m)!!]^2} \left(F\frac{b}{r}\right)^{2m} \frac{1}{(m+2)(m+1)} \left[2(m+1) - \frac{9}{(1-2\nu)}\right]$$

(E-10b)

$$+ \frac{1}{420}(p_1-1)\left(F\frac{b}{r}\right)^2(1-s_n\cos^2\lambda_n) \sum_{m=0}^{\infty} \frac{1}{[(2m)!!]^2} \left(F\frac{b}{r}\right)^{2m} \frac{1}{(m+2)(m+1)} \left[7m+12 - \frac{9}{(1-2\nu)}\right] \quad ,$$

$$T_3^{\varepsilon} = \frac{1}{3}T_3 + \frac{1}{840}\frac{1}{(1-2\nu)^2}(p_1-1)^2(F\frac{b}{r})^2(1-s_n\cos^2\beta_n)\sum_{m=0}^{\infty}\frac{1}{[(2m)!!]^2}(F\frac{b}{r})^{2m}\frac{1}{(m+2)(m+1)}$$

$$\cdot\,[(1-2\nu)^2(2m+1)(m+1) - 6(1-2\nu)(2m+1) + 3(m-1)] \qquad \text{(E-10c)}$$

$$+\frac{1}{1680}\frac{1}{(1-2\nu)^2}(p_1-1)^2(F\frac{b}{r})^2(1-s_n\cos^2\lambda_n)\sum_{m=0}^{\infty}\frac{1}{[(2m)!!]^2}(F\frac{b}{r})^{2m}$$

$$\cdot\,\frac{1}{(m+2)(m+1)}[(1-2\nu)^2(2m+3)(2m+1) - 6(1-2\nu)(2m+1) + 12m + 15] \quad .$$

Substituting equations (E-10) into equation (E-4), we arrive at the final result:

$$g'(r) = \frac{3}{10}\beta P(p_1-1)[H^E\frac{b^2}{r^2}(1-s_n\cos^2\beta_n)+(1+H_\lambda^E\frac{b^2}{r^2})(1-s_n\cos^2\lambda_n)+0(r^{-4}) \qquad \text{((E-11)}$$

where

$$H_\beta^E = \frac{\beta^2P^2}{112(1-\nu)^2\pi^2}[7(1-2\nu)^2-(7-10\nu-8\nu^2)(p_1-1)-(2-2\nu-\nu^2)(p_1-1)^2] \qquad \text{(E-12)}$$

and

$$H_\lambda^E = \frac{\beta^2P^2}{224(1-\nu)^2\pi^2}[21(1-2\nu)^2+(3-30\nu+48\nu^2)(p_1-1)+3(1+\nu^2)(p_1-1)^2] \quad . \qquad \text{(E-13)}$$

Note that the sum of the first terms in equations (E-10a), (E-10b), and (E-10c) cancel the fourth term of equation (E-4).

REFERENCES

E.1 I.F. Gradshteyn and I.M. Ryzhik, "Table of Integrals, Series and Products", Academic Press, New York (1965), 4th Edition.

APPENDIX F

EVALUATION OF g'(r) FOR A SCREW DISLOCATION

g'(r) for a screw dislocation is given by

$$g'(r) = \frac{9}{2}\beta P(p_1-1)\int\frac{d\Omega_h}{4\pi}\int_0^{2\pi}\frac{d\theta_r}{2\pi}(\hat{r}\cdot\hat{h})^2(s_n t_i^{(n)} t_j^{(n)}\hat{h}_i\hat{h}_j-1)\exp[-\beta E_s^i(\underset{\sim}{r},\hat{\underset{\sim}{h}})] \quad , \tag{F-1}$$

$$g'(r) = \frac{9}{2}\beta P(p_1-1)\{\int\frac{d\Omega h}{4\pi}\int_0^{2\pi}\frac{d\theta_r}{2\pi}(\hat{r}\cdot\hat{h})^2(s_n t_i^{(n)} t_j^{(n)}\hat{h}_i\hat{h}_j-1)\exp[-\beta E_s^i(\underset{\sim}{r},\hat{\underset{\sim}{h}})] \quad , \tag{F-2}$$

$$- \frac{1}{3}g(r)\Big|_{\varepsilon=0}\} \quad .$$

Substituting for $E_s^i(\underset{\sim}{r},\hat{\underset{\sim}{h}})$ (equation 38) equation (F-2) becomes

$$g'(r) = \frac{9}{2}\beta P(p_1-1)\{\int\frac{d\Omega_h}{4\pi}\int_0^{2\pi}\frac{d\theta_r}{2\pi}(\hat{r}\cdot\hat{h})^2 s_n t_i^{(n)} t_j^{(n)}\hat{h}_i\hat{h}_j\exp(\tfrac{1}{6}A\tfrac{b}{r}G_{\mu\nu}\hat{r}_\mu\hat{h}_\nu\hat{h}_3) \tag{F-3}$$

$$- \frac{1}{3}g(r)\Big|_{\varepsilon=0}\} \quad .$$

where A is given by equation (D-2) is Appendix D. Expanding the exponential in an infinite series, we obtain

$$g'(r) = \frac{9}{2}\beta P(p_1-1)\{\frac{1}{2\pi}s_n t_i^{(n)} t_j^{(n)}\int_0^{2\pi}\hat{r}_\mu\hat{r}_\nu\gamma(\mu,\nu,i,j)d\theta_r$$

$$+ \frac{1}{2\pi}s_n t_i^{(n)} t_j^{(n)}\sum_{m=1}^{\infty}\frac{1}{m!}(\tfrac{1}{2}A\tfrac{b}{r})^m\int_0^{2\pi}G_{\mu_1\nu_1}G_{\mu_2\nu_2}\cdots G_{\mu_m\nu_m} \tag{F-4}$$

$$\cdot\hat{r}_\mu\hat{r}_\nu\hat{r}_{\mu_1}\hat{r}_{\mu_2}\cdots\hat{r}_{\mu_m}\gamma(\mu,\nu,i,j,\nu_1,\nu_2,\ldots,\nu_m,\overbrace{3,3,\ldots,3}^{m})d\theta_r - \frac{1}{3}g(r)\Big|_{\varepsilon=0}\} \quad .$$

The γ values can be determined using the solution in Appendix B of reference 16(a) and using the identities given by equation (37), equation (F-4) reduces to

$$g'(r) = 36\beta P(p_1-1)(1-s_n\cos^2\lambda_n) \sum_{m=0}^{\infty} \frac{(1-m^2)[(2m+1)!!]^2}{(2m+1)(4m+5)!} \left(A\frac{b}{r}\right)^{2m} \qquad \text{(F-5)}$$

where $(2m+1)!!$ is given by equation (D-5) of Appendix D and

$$t_3^{(n)} = \cos \lambda_n \qquad \text{(F-6)}$$

where λ_n is the angle between the line direction of the screw dislocation and the nth principal direction of the externally applied stress.

APPENDIX G

THE CYLINDRICAL SYMMETRIZATION PROCEDURE

Here we examine the accuracy of the cylindrical symmetrization procedure and the approximations involved in neglecting $O(r^{-4})$ in equations (31) and (39). The boundary value problem that results from applying the extremum principle to equation (4), with K(r)=0, can be solved exactly for an isotropic point defect in the strain field of an edge dislocation. The resulting expression for the sink strength per unit line length, ζ, is [23]

$$\zeta = 2\pi I_o(L\frac{b}{r_o}) / [K_o(L\frac{b}{R}) \cdot I_o(L\frac{b}{r_o}) - K_o(L\frac{b}{r_o}) \cdot I_o(L\frac{b}{R})] \qquad (G\text{-}1)$$

where I_o and K_o are the modified Bessel functions of zero order and

$$L^2 = F \ (p_n=1, \ n=1,2,3),$$
$$L = \frac{\beta P \ (1-2\nu)}{4\pi \ (1-\nu)} \cdot \qquad (G\text{-}2)$$

Following the cylindrical symmetrization procedure and putting $p_1=1$ in equation (29), we have

$$g(r) = \int_o^{2\pi} \frac{d\theta_r}{2\pi} \exp(-2L\frac{b}{r}\sin\theta_r)$$
$$= \sum_{n=0}^{\infty} (n!)^{-2} L^{2n} (\frac{b}{r})^{2n} \cdot \qquad (G\text{-}3)$$

Equation (15) can then be numerically evaluated using as many terms of equation (G-3) as desired, and compared with equation (G-1) to determine the magnitude of the error introduced by the cylindrical symmetrization procedure. In addition, we will compare the results in equation (31), setting $p_1=1$ in equation (32), with equation (G-1). The results for two example sets of parameters are listed in Table G-1. We choose the capture

radius to be equal to b. The values of ν and b are those for fcc copper. The value of 70 eV for $Tr(P_{ij})$ is an upper limit on the values used in the actual calculation (see Table 1). The first set of temperature and dislocation density values are those for the "worst" case in terms of error. Two facts immediately become obvious. First, the cylindrical symmetrization procedure overestimates the sink strengths. Second, two terms of the series give a better result than the sum to convergence (to 10^{-6}) of the entire series. The partial sums of the series, in equation (G-3), is monotonically increasing. Since the first two terms of the series yield a result that already exceeds the exact result, adding more terms will increase the error. This makes neglecting terms of $O(r^{-4})$ and higher mandatory in the anisotropic case. In addition to these results, we note that overestimation will occur for both ζ_i and ζ_v. Since B is proportional to the difference of these two parameters, some of the error will be cancelled. Finally, we note that the error, $\lesssim$ 6.5% in the cylindrical symmetrization procedure, is probably less than the accuracy with which the elements of the dipole tensor are known. At any rate, we feel that the accuracy is good enough to give us a good physical picture of the shape effect on point-defect migration to a straight dislocation.

TABLE G-1

COMPARISON OF THE EDGE DISLOCATION SINK STRENGTH FOR ISOTROPIC POINT DEFECTS WITH THE EXACT SOLUTION

$Tr[P^s_{ij}]$ (eV)	ν	$r_o=b$ (nm)	TEMP. (K)	ρ (cm/cm^3)	L	ζ EXACT SOLUTION	ζ SERIES			
							Sum To Convergence	% Error	Two Terms Only	% Error
70	0.343	0.2556	300	10^{10}	34.3	3.15	3.71	17.9	3.36	6.5
70	0.343	0.2556	500	10^{8}	20.6	1.31	1.40	6.6	1.34	2.5